# *Elaia, Pergamon's maritime satellite*

Seeliger, Martin; Pint, Anna; Feuser, Stefan; Riedesel, Svenja; Marriner, Nick; Frenzel, Peter; Pirson, Felix; Bolten, Andreas; Brückner, Helmut

*Published in:*
Journal of Quaternary Science

*DOI:*
10.1002/jqs.3091

*Publication date:*
2019

*Citation for published version (APA):*
Seeliger, M., Pint, A., Feuser, S., Riedesel, S., Marriner, N., Frenzel, P., Pirson, F., Bolten, A., & Brückner, H. (2019). Elaia, Pergamon's maritime satellite: The rise and fall of an ancient harbour city shaped by shoreline migration. *Journal of Quaternary Science*, *34*(3), 228-244. https://doi.org/10.1002/jqs.3091

Martin Seeliger[1]*, Anna Pint[2], Stefan Feuser[3], Svenja Riedesel[4], Nick Marriner[5], Peter Frenzel[6], Felix Pirson[7], Andreas Bolten[2] & Helmut Brückner[2]

# Elaia, Pergamon's maritime satellite: the rise and fall of an ancient harbour city shaped by shoreline migration

[1] Department of Physical Geography, Faculty of Geosciences, Goethe-University Frankfurt, Germany
[2] Institute of Geography, University of Cologne, Germany
[3] Institute of Classical Studies, Kiel University, Germany
[4] Department of Geography and Earth Sciences, Aberystwyth University, United Kingdom
[5] CNRS, Laboratoire Chrono-Environnement UMR 6249, Université de Bourgogne-Franche-Comté, France
[6] Institute of Earth Sciences, Friedrich-Schiller University Jena, Germany
[7] German Archaeological Institute (DAI), Istanbul, Turkey

*Corresponding author: seeliger@em.uni-frankfurt.de (Martin Seeliger)

**Running title: Shoreline Migration Elaia**

**Keywords: Palaeogeography, coastal evolution, Micropalaeontology, Aegean, Sea-level fluctuations**

## Abstract

Throughout human history, communication and trade were key to societies. Because maritime trade facilitates the rapid transportation of passengers and freight at relatively low costs, harbours became hubs for traffic, trade, and exchange. This general statement holds true for the Pergamenian kingdom, which ruled wide parts of today's western Turkey during Hellenistic times. Its harbour, located at the city of Elaia on the eastern Aegean shore, was used extensively for commercial and military purposes.

This study reconstructs the coastal evolution in and around the ancient harbour of Elaia and compares and contrasts the observed environmental modifications with archaeological and historical findings. We used micropalaeontological, sedimentological, and geochemical proxies to reconstruct the palaeoenvironmental dynamics and evolution of the ancient harbour. The geoarchaeological results confirm the archaeological and historical evidence of Elaia's prime during Hellenistic and early Roman times, and the city's gradual decline during the late Roman period. Furthermore, our study demonstrates that Elaia holds a unique position as a harbour city during ancient times in the eastern Aegean region, because it was not completely influenced by the high sediment supply associated with river deltas. Consequently, no dredging of the harbour basins is documented, creating exceptional geo-bio-archives for palaeoenvironmental reconstructions.

## Introduction

Around the end of the Holocene marine transgression, circa 6000 BP (Lambeck, 1996; Lambeck and Purcell, 2007), sea-level stabilisation enabled ancient societies to settle along Mediterranean shores (Anthony *et al*., 2014; Murray-Wallace and Woodroofe, 2014; Vacchi *et al*., 2014, 2016a; Khan *et al*., 2015; Benjamin *et al*., 2017; Seeliger *et al*., 2017). For many civilisations, a connection to the sea was an important factor in establishing a flourishing settlement. In the Aegean, this statement is, for example, supported by the Neolithic settlements of Hoca Çeşme in Thrace (Başaran, 2010; Özbek, 2010), Hamaylıtarla on the Gallipoli peninsula (Özbek, 2010) and Çukuriçi Höyük near ancient Ephesus (Horejs, 2012; Horejs *et al.*, 2015; Stock *et al*., 2015). All of them were situated less than 4 km from the sea, much closer than they are today (Ammerman *et al*., 2008). There are many examples from the Aegean that demonstrate that the fate of ancient settlements was closely linked to migrating shorelines and changing sea level. In Western Anatolia, Troy, Miletos, Ainos, Ephesus, and Liman Tepe are the most prominent ones. Their rise and fall as harbour cities were shaped essentially by environmental changes, which have been described by many geoarchaeological studies (Kraft *et al*., 1977, 2007; Kayan, 1999, 2014; Brückner *et al*., 2006, 2013, 2015; Goodman *et al*., 2008, 2009; Delile *et al*., 2015; Shumilovskikh *et al*., 2016; Seeliger *et al*., 2018).

Here, we investigate the evolution of the coastal configuration around the city of Elaia that hosted the former military and commercial harbour of ancient Pergamon in Hellenistic and Roman times. Since 2013, several papers have focused on the environmental evolution of the Bay of Elaia. By analysing sediment cores taken inside and outside the main harbour basin of Elaia, the closed harbour, Seeliger *et al*. (2013) demonstrated how it was built in the first half of the 3rd century BC, how it has been used during the apogee of Elaia, and why it was abandoned due to massive sedimentation in late Roman times (Fig. 2). Seeliger *et al.* (2014) used optically stimulated luminescence (OSL) dating and electrical resistivity tomography (ERT) measurements to probe the construction style and age of presently submerged walls circa 1–2 km south of the city and interpret these structures as the remains of saltworks constructed using spolia in Late Antiquity, a time when the harbours of Elaia were no longer navigable and the people had abandoned the city (Fig. 2a). Pint *et al.* (2015) performed detailed analyses of foraminifera and ostracoda, in combination with 3D-ERT measurements, to detect the style and usability of presumed Hellenistic ship sheds in the open harbour area of Elaia. They concluded that the open harbour and its ship sheds were operational during Hellenistic times, but were no longer navigable from Roman Imperial times onwards.

Furthermore, Shumilovskikh *et al*. (2016) undertook a palynological investigation of sediment core Ela 70, taken from inside the closed harbour basin. This work precisely reconstructed the palaeoenvironmental conditions and the vegetation history of the Bay of Elaia during the last 7500 a. Finally, Seeliger *et al.* (2017) described a new sea-level indicator based on foraminifera associations in the context of the transgressive contact. Based on these data, they reconstruct a relative sea-level (RSL) history for the area showing steadily rising sea-level since 7500 BP and today's sea-level maximum. By comparing and contrasting their RSL history to curves from nearby Greek sites in the Aegean they reviewed the RSL evolution of the Aegean since the mid-Holocene. Furthermore, Feuser *et al.* (2018) recently published a summary presenting the state-of-the-art knowledge on the use of the Elaia's harbours, from an archaeological perspective.

In this article, we aim to integrate key findings of previous studies with new chronostratigraphic results to (i) investigate the causes of environmental modifications; (ii) to reconstruct the changes in the shoreline of the Bay of Elaia; and (iii) to provide fresh insights into the link between shoreline changes and human-environment interactions during Elaia's settlement period. Therefore, we focus on the time period from 1500 BC onwards, which covers Elaia's prime as Pergamon's prospering harbour. In addition, we compare our results with other ancient coastal settlements in Asia Minor to furnish a broader view on different environmental changes, which shaped the rise and fall of ancient coastal settlements in the eastern Aegean.

## Physical setting

Elaia is located in the north-western part of modern Turkey (Figs. 1a, b). The study area is part of the westwards drifting Aegean-Anatolian microplate (Vacchi *et al.*, 2014). As a consequence of this drift, several E-W oriented rift structures were formed in the late Miocene, such as the Bergama graben, and its tributary, the Zeytindağ graben. This tectonic ensemble represents a fractured zone, which was favourable to the evolution of the Kaikos valley (Vita-Finzi, 1969; Aksu *et al*., 1987; Seeliger *et al*., 2013; Fig. 1a). The Karadağ Mountains to the west and the Yuntdağ Mountains to the east border the Gulf of Elaia (Figs. 1, 2). The wide alluvial plain and the cuspate delta of the Bakır Çay (ancient name: Kaikos) are located to the west of the Bay of Elaia, separated by the flat ridge of Bozyertepe (40 m a.s.l. (above present sea level; Fig. 2)).

The Elaia coastal zone has a typical Mediterranean climate, Csa according to Koeppen and Geiger's nomenclature, with hot and dry summers, and mild and humid winters (Yoo and

Rohli, 2016). Therefore, heavy rain and torrential rivers are major morphological agents (Brückner, 1994; Jeckelmann, 1996). Our own observations confirmed that the sea in the Bay of Elaia turns brownish due to excessive wash-down of colluvial material during heavy rain. Due to the steepness of the Yuntdağ Mountains, this effect is even stronger in the eastern part of the Bay of Elaia (Fig. 2c).

## Historical background

Pergamon is one of the most famous ancient settlements in Turkey, frequently mentioned with Troy, Miletos, Ainos, and Ephesus (Kraft *et al.*, 1980, 2003, 2007; Kayan, 1999; Brückner *et al.*, 2013; Seeliger *et al.*, 2018). Thanks to shifts in the settlement areas, its impressive monumental structures, its important library and school of philosophers, Pergamon provides detailed insights into the urban structure of a Hellenistic city (Radt, 2016). Soon after Alexander the Great died in Babylon in 323 BC, the so-called "Wars of the Diadochi" affected great tracts of his empire (Cartledge, 2004). In a later stage of these fights, the dynasty of the *Attalids* came to power in the Kaikos region and established – in alliance with Rome – a powerful kingdom in Asia Minor, which, during its prime under King Eumenes II (197–159 BC) ruled the western half of present-day Turkey. In 133 BC, their realm was integrated into the growing Roman Empire (Hansen, 1971; Pirson and Scholl, 2015; Radt, 2016; Fig. 1c). Pergamon's location on top of the 330 m high Acropolis hill, overlooking the surrounding Kaikos plain, was excellent for security and defence, but complicated trade and transport. Furthermore, the Pergamenians were in need of a maritime harbour. They found it in the nearby city of Elaia, located on the Aegean Sea approximately 26 km south-west of Pergamon (Figs. 1a, 2a). According to current research knowledge, Elaia came under Pergamenian hegemony during the regency of Eumenes I (263–241 BC; Pirson, 2004; Radt, 2016). Additionally, *Strabo* mentioned Elaia as the commercial harbour of the Pergamenians and as the military base of the *Attalids* (*Geographica XIII, 1, 67; XIII, 3, 5*). Further evidence from literary sources and archaeological findings emphasises the close link between Elaia and Pergamon (Pirson, 2004, 2008, 2010, 2011, 2014). The harbour zone of Elaia was divided into three parts (Fig. 2).

First, the closed harbour basin (I in Fig. 2) within the fortification walls, which was built in early Hellenistic times. It was protected from the sea and enemies by two massive breakwaters; nowadays they are landlocked, but still visible. Geoarchaeological research has revealed that substantial siltation occurred between the 3rd and the end of the 4th centuries AD; from the 5th century AD onwards the closed harbour was no longer navigable (Pirson, 2007, 2008; Seeliger *et al*., 2013, 2017). Second, a circa 250 m long open harbour zone (II in Fig. 2) stretching from the southern breakwater of the closed harbour south-eastwards to the point where an internal wall reached the waterfront. This so-called *diateichisma* divided the city area into a northern, densely-populated part and a southern one (Pirson, 2011; Pint *et al*., 2015). Third, a beach harbour extended from south of the diateichisma to the south-eastern tip of the city wall (III in Fig. 2). This area was probably used as a multifunctional military zone, including dockyards where warships were beached and maintenance work was conducted (Pirson, 2011, 2014; Pint *et al*., 2015).

Palaeogeographical research was conducted to assess small-scale palaeoenvironmental changes in the Bay of Elaia. Because Elaia served as the satellite harbour city of Pergamon during its prime, previous research focussed on the function and temporal use of the different harbours identified (Seeliger *et al*. 2013, 2017; Pint *et al*. 2015). Although detailed research was conducted, some key questions remain. Key knowledge gaps include: (i) How did coastal and RSL changes influence the human occupation history of the city? (ii) To what extent does Elaia fit with the traditional "rise and fall model" linked to shoreline migration?

Seeliger *et al*. (2017) took a first step toward answering these questions, by publishing a RSL curve for Elaia and comparing it to the RSL histories of other study areas in the Aegean. Here we seek to further explore the role of Elaia as an example of shoreline migration and human settlement changes in the Aegean during ancient times. This research is based on 19 sediment cores, drilled along five transects perpendicular to the present shoreline (Fig. 2a). This approach has been widely adopted in Mediterranean coastal studies (e.g. Kraft *et al*., 2007; Goodman *et al*., 2008, 2009; Kayan, 2014; Marriner *et al*., 2014; Delile *et al*., 2015, Morhange *et al*., 2016; Evelpidou *et al*., 2017; Flaux *et al*., 2017; Giaime *et al*., 2017; Pennington *et al*., 2017; Seeliger *et al*., 2018) to investigate lateral and vertical changes in the sediment stratigraphy and to probe the evolution of the landscape, notably shoreline migration.

## Material and methods

### *Geoarchaeological fieldwork*

Sediment cores were extracted using an Atlas Copco Cobra TT vibracorer with open steel auger heads (diameter: 6 and 5 cm, respectively) in the surroundings of the Bay of Elaia, down to a maximum depth of 12 m b.s. (below the surface). On-site, sediments were described according to grain size and colour (Ad-hoc-AG Boden, 2005; Munsell Soil Color Charts) and bulk samples for laboratory analyses were taken from the open sediment cores

(5–6 samples/metre). All coring sites were georeferenced using a Leica DGPS System 530 (accuracy of ≤2 cm in all three dimensions; Seeliger *et al*., 2013, 2014); they are reported in m above sea level (a.s.l.) and m below the surface (b.s.).

### *Sedimentology and geochemistry*

Multi-proxy laboratory analyses were conducted (Ernst, 1970; Hadler *et al*., 2013; Bartz *et al*., 2015, 2017; Seeliger *et al*., 2013, 2018). Samples were air-dried and sieved to separate the ≤2 mm grain-size fraction for further analyses. For laser-based grain-size analysis (Beckman Coulter LS13320), the organic content was decomposed using 15 % hydrogen peroxide ($H_2O_2$). Afterwards, sodium pyrophosphate ($Na_4P_2O_7$; concentration: 47 g/l) was taken as a dispersant. Each sample was measured three times in 116 classes, determining grain-size distributions in a range from 0.04 to 2000 µm. For the calculation of grain-size parameters (Folk and Ward, 1957), we used the software package GRADISTAT (Blott and Pye, 2001)._To estimate the organic content, measurements of LOI (loss on ignition) were performed by oven drying (105 °C for 12 h to determine the water content) and combustion in a furnace (550 °C for 4 h to determine the organic substance). Electric conductivity was measured in an aqueous solution (5 g sediment in 25 ml deionised water) with a glass electrode connected to a Mettler Toledo InLab®731-2m instrument. To determine different sedimentary units, characteristic elements (e.g. Fe, K, Ca, Ti, etc.) were measured using a portable XRF (X-ray fluorescence) spectrometer (Niton Xl3t 900 GOLDD; Vött *et al*., 2011; Lubos *et al*., 2016). To ensure comparability with all XRF analyses and to reduce grain-size dependency, each sample was ground to powder in a ball triturator (Retsch PM 4001) and then pressed into pills.

### *Micropalaeontology*

For microfaunal analysis, selected 1 cm³ samples were wet-sieved using a 100 µm mesh. Under a stereoscopic microscope, at least 300 ostracod valves and foraminifer tests, respectively, were picked from appropriate splits of the residues of every sample. If less than 300 specimens were present within a sample all were picked. Species were identified and counted according to Bonaduce *et al*. (1975) and Joachim and Langer (2008) for ostracods as well as Cimermann and Langer (1991), Meriç *et al*. (2004), and Murray (2006) for foraminifers.

### *Chronology*

The chronological framework is based on $^{14}$C-AMS age determinations. Depending on the $\delta^{13}$C-value, each sample was calibrated using either the IntCal13 or the MARINE13 calibration curve in Calib 7.1 (Reimer *et al.*, 2013) with a marine reservoir age of 390±85 a and a ΔR of 35±70 a (Siani *et al.,* 2000). Siani *et al.,* (2000) used shells of known age sampled in the Dardanelle Strait and stored in the Muséum National d'Histoire Naturelle, Paris to calculate the local marine reservoir age and its ΔR. As there are no further studies in the closer vicinity of Elaia, this value has been chosen to correct the calibrations on marine material. Finally, because the spatio-temporal variation of the marine reservoir effect for the Aegean is still not completely understood, the $^{14}$C-ages of marine carbonates should be interpreted carefully. Because this paper presents archaeological-related data, all ages are presented in cal a BC/AD. Tab. 1 provides all mentioned ages in cal a BP.

## Results of Ela 57 and Ela 12

The coring profiles of the Elaia region, a selection of 19 is presented here (Fig. 2a), can be divided into two groups: those, which reach bedrock and those that do not. Additionally, the sedimentation pattern in the western part of the Bay (transects A–A' and B–B') differs significantly from that of the eastern part (D–D', E–E', and F–F'). This is demonstrated by the detailed description of two cores, one from each group: Ela 57 (Figs. 3, 4) and Ela 12 (Figs. 5, 6). Additionally, Ela 58 (Pint *et al.*, 2015) is considered in order to present all sedimentary units (Fig. 2a). A detailed description of the profiles Ela 57 and Ela 12 is stated in Appendix 1.

## Interpretation

### *Introduction of sedimentary units*

Many sediment cores from the Elaia area are summarised by the classification in units of typical environmental characteristics. Their definition based on geochemical, granulometric, and micro-faunistic parameters of cores Ela 57 and 12. This compilation is intended to shorten the interpretation of the cores (Fig. 7) and described in detail in Appendix 2.

### *Sediment core-based reconstruction of palaeoenvironments*

Based on the previous sections, coring profiles Ela 57 and Ela 12 are interpreted as follows:

*Sediment core Ela 57 representing the eastern part of the Bay of Elaia*

The palaeogeographical evolution of the eastern part of the Bay of Elaia is exemplified by Ela 57 (Figs. 2, 3, 4).

Neogene bedrock (unit 1), encountered at 5.42 m b.s., forms the base of numerous cores in the study area. The calcareous sandstone, outcropping nearby, was used to construct the harbour breakwaters (Seeliger *et al.*, 2013, 2014). The overlying unit 2 represents the transgressive littoral unit during the Holocene sea-level rise. The high-energy environment is obvious from a number of gravels, the coarse grain size, and patches of seagrass. The low biodiversity and the sole occurrence of robust foraminifers in the lower part of unit 2, such as *Ammonia compacta* and *Elphidium crispum*, are evidence for the high-stress level of this littoral environment in which only a few species are able to survive (Seeliger *et al.*, 2017). The fining-upward sequence is due to increasing water depth, which is also reflected by a higher biodiversity. The Holocene transgression reached this area at the end of the 3rd millennium BC (2198–2035 cal a BC), which is far before the human occupation phase of Elaia. The second age of Ela 57 dates to late Hellenistic/ early Roman times (165 cal a BC–1 cal a BC/AD), the period when Elaia flourished. Rising sea level led to the formation of a shallow water body represented by unit 4. It shows a fining-upward sequence due to the inland migration of the shoreline, leading to reduced wave action. This results in a lower amount of shell debris and the occurrence of preserved valves. The microfaunal association indicates a shallow marine environment. Based on our results from inside the closed and open harbours, relative sea level at the turn of the eras was approximately 1.50 m lower than today. Thus, water depth at this time should not have exceeded more than 1.30–1.50 m (Pint *et al.*, 2015; Seeliger *et al.*, 2017).

By then, the surroundings of this part of the city area may have served as a beach harbour area where foreign soldiers landed and repaired their ships and put up camp, thus staying outside the actual city area. This custom was normal for small to medium-sized cities at this time, because it offered a higher level of security for the inhabitants. As the nearby coring Ela 56 does not show any marine or littoral sediments, the site of Ela 57 always lay in a nearshore position, close to the landing area for ships and smaller vessels. A sharp contact at -1.61 m a.s.l. suggests a sudden end to this sheltered marine water body, possibly due to a massive deposition engendered by torrential floods, triggered by heavy rainfall. Such erosional events were favoured by the widespread deforestation of this area during Hellenistic and Roman times (Shumilovskikh *et al.*, 2016). The erosional contact at the base, the fining-upward sequence, the fluvial character of the stratum including brick fragments, seeds, charcoal, and even bones, all washed down from the nearby slopes, as well as the absence of microfauna, support this interpretation. The upper part of this unit dates to Roman Imperial times. Since the dated olive stone (Ela 57/8H; Tab. 1) is very robust and may have been reworked, the age should only be regarded as a minimum age. It seems that the fluvial deposition most probably occurred during the final phase of the settlement of Elaia in late Roman times which may have influenced the final decision to abandon the city. Since the area around coring site Ela 57 suddenly became terrestrial, the second transition of the shoreline, often indicated by a second littoral phase (unit 5), is missing. That the area was at least partly influenced by human impact is evidenced by the anthropogenically-disturbed colluvium (unit 7b), which forms the top layer.

### *Sediment core Ela 12 representing the western part of the Bay of Elaia*

The palaeogeographical evolution of the western Bay of Elaia is exemplified by profile Ela 12 (Figs. 2, 5, 6).

At the bottom, the profile shows sediments of a sheltered embayment (unit 4) where *Posidonia oceanica* meadows could thrive on the sea floor (Vacchi *et al.*, 2016b). Well-preserved marine bivalves support this idea. The geochemical data and the microfaunal association indicate a near-shore environment as typically open marine species are missing (Pint *et al.*, 2015). A radiocarbon age of 803–568 cal a BC dates this part to the first half of the 1st millennium (Geometric-Archaic times). Very little is known about the history of the study area during this period (Pirson and Scholl, 2015; Fig. 1c). The shallow marine environment prevailed for some time until sediments from the nearby Bozyertepe were increasingly washed into the embayment. This caused a regression of the shoreline with decreasing water depth, and the establishment of littoral unit 5, which is of progradational origin. Compared to the transgressive unit 2 of Ela 57, the progradational unit 5 of Ela 12 has a similar microfaunal composition but displays a coarsening-upward sequence. The environmental stress led to low biodiversity, while the increased occurrence of mollusc and shell debris provides evidence of intense wave energy. It can be excluded that the advancing delta of the Kaikos (Bakır Çay) played a major role in the silting up of this inner part of the Bay of Elaia because neither Ela 12 nor the whole transects A–A’ and B–B’ contains fluvial-deltaic sediments and the Bozyertepe acts as a barrier for this material (Fig. 2a). The littoral unit ends at -2.78 m a.s.l., when terrestrial processes become dominant. This is the onset of the accumulation of colluvium (unit 7a). Since transect A–A’ is situated at a distance from the settled area of Elaia, it is not surprising that no direct indicators of human impact are found inside the colluvium.

*Landscape evolution based on coring transects*

After the detailed description of two representative sediment cores, five transects and one single coring are discussed to clarify the landscape evolution of the Bay of Elaia (Fig. 8). Transect A–A' consists of three different types of profiles. The coastal corings Ela 11 and 12 show a typical regressive sedimentary sequence (Fig. 8). Increased sedimentation in the context of the settlement period of Elaia led to the silting up of a low energy, shallow marine water body (unit 4), which turned to a littoral progradation unit 5 and later to a natural colluvial environment (unit 7a). Ela 14 and 20 reach the bedrock, which is topped by nearshore littoral deposits (unit 2); these are overlain by natural colluvium. The rising bedrock towards the Bozyertepe causes the landward thinning of the littoral strata. Since core Ela 19 does not contain marine, fluvial, or littoral units, the maximum marine transgression in A–A' is close to coring Ela 20, where it is dated to the end of the 2nd millennium BC. Transect B–B'represents the marine transgression into the valley between the Acropolis to the east and the Bozyertepe to the west (Fig. 8). It provides results comparable to A–A'. Coastal corings Ela 1 and 2 demonstrate a regressive sediment sequence, similar to Ela 11 and 12. They represented a shallow water body in this area of the Bay of Elaia at least since the first half of the 1st millennium BC. According to these results, the areas of Ela 1 and 2 were still under marine influence during the main occupation phase of Elaia (Figs. 1c, 2). Since Ela 9 only shows colluvial sediments, coring Ela 3/17 marks the maximum marine transgression of B–B'. This dates to the end of the 3rd millennium BC. Ela 58 ("C") is the only core in this area, which includes a shallow marine unit (unit 3) with high biodiversity. It dates to the 4th/5th millennia BC. As in the eastern transects, massive fluvial input ended the shallow marine conditions and initiated a sheltered water area (unit 4), which prevailed throughout Elaia's prime. Later, the Elaitians dumped material in this area to consolidate the terrain. Transects D–D', E–E', and F–F' show similar results, and are therefore presented together. The nearshore coring profiles (Ela 59, 55, and 62) reach the bedrock. The transgressive littoral unit 2, starting with an erosional disconformity, is covered by unit 4 of a stagnant marine water body. Obviously, the very low-energy wave conditions prevailed because a progradational unit 5 is missing; all of the profiles show a smooth transition to colluvial deposits (unit 7a). The inland corings (Ela 60, 56, and 64) reveal a terrestrial sedimentation pattern interrupted by a layer of fluvial sediments, most probably caused by torrential floods. The central corings (Ela 61, 57, and 63) contain key information about the marine extension in this area. All of them display a typical stratigraphy: the bedrock is overlain by transgressive littoral deposits; then units of a low-energy marine embayment follow and provide evidence of the rising sea level. The shallow marine deposit is covered by massive input of fluvial sediments, which are topped by human-induced colluvium. Severe flooding can only be traced in the sediment sequence of the central and inland corings (Seeliger *et al*., 2017).

*Synopsis*

With regard to the height above sea level in F–F', a similar age for the maximum marine ingression in each transect of circa 1500 BC is assumed. Derived from the thickness of the marine strata of Ela 58 ("C"), the maximum transgressive shoreline is probably located further inland, i.e. in the area of the later city (where coring was impossible). Ela 61 indirectly proves this assumption. This is comparable to other ancient cities such as Miletos, Ainos, and, Ephesus where parts of the cities were also erected on former marine sediments (Brückner *et al*., 2006, 2015; Kraft *et al*., 2007; Seeliger *et al*., 2018). The eastern city district transects and Ela 58 ("C") show thick sheet-wash deposits which caused massive siltation of the area. In the case of Ela 58, this could have taken place at the beginning of the 1st millennium BC. This is in good accordance with transect D–D' where this event occurred at a similar date (Ela 61/16; 1149–791 cal a BC). In Ela 57 (E–E'), it is visible just around the turn of the eras, whereas in Ela 63 (F–F') it occurred in Classical or even Hellenistic times (shortly after Ela 63/10/H; 797–551 cal a BC). However, severe flood events did not occur in the western part of the embayment (transects A–A' and B–B'). In sum, torrential floods associated with sheet-wash dynamics occur before and during the intense human settlement activity; they affected the eastern area of ancient Elaia (Fig. 2). This is, on the one hand, a result of the topography of the nearby foothills of the steep Yuntdağ Mountains, as compared to the flat Bozyertepe and the Acropolis (A–A' and B–B'; Fig. 2). On the other hand, the human influence in the eastern area of the embayment was more intense, leading to degradation of the vegetation cover, soil degradation, and erosion. At the end of the 1st century BC and the beginning of the 1st century AD the settlement pattern of the surroundings of Elaia changed when several of the Hellenistic farmsteads were abandoned – maybe because of intense floods (Pirson, 2011).

*Scenarios of shoreline changes*

Based on these results, we reconstructed the palaeogeography of the Bay of Elaia for three different time periods (1500 BC, 300 BC, and AD 500; Figs. 2, 9).

**1500 BC:** This is the time of the maximum marine extension in the Bay of Elaia, when sea level was 3.3–2.4 m lower than today (Seeliger *et al*., 2017). The coastal zone reached northwards along the slopes of Bozyertepe, almost up to Ela 9 where one of Elaia's cemeteries was located (Pirson, 2010). This supports the idea that the sea never transgressed this area during the Holocene. During the maximum marine extension, the later Acropolis of Elaia protruded into the bay as a peninsula. Nonetheless, it was most probably uninhabited at this time. The small embayment to the north of Ela 58 may have acted as a preferred landing area, but as yet this assumption has not been verified by archaeological finds. The same holds true for the western flank of the Acropolis. In the eastern city area, the shoreline lay close to the foothills of the Yuntdağ. The former shallow marine and littoral areas of the later city are easy to identify. Once these had been silted up, and probably also partly filled in by the inhabitants, they evolved into settled ground after circa 500 BC (Figs. 2, 9).

**300 BC:** This scenario represents the period when Elaia started to prosper, when sea level was just 1.6–2.0 m lower than today (Seeliger *et al.*, 2017). Archaeological findings document intense human activities on the Acropolis and in the eastern city district (Pirson, 2010). In addition, palynological data show that various crops were intensively cultivated in the surroundings of Elaia (Shumilovskikh *et al.*, 2016).

Increased sediment load due to soil erosion from Bozyertepe and minor activities of a nameless ephemeral creek between Bozyertepe and Acropolis caused a shoreline regression in the western part. None of the corings of A–A' and B–B' show fluvial sediments of the nearby Kaikos delta. Therefore, its influence concerning the siltation of the inner part of the Bay of Elaia can be neglected. Wide areas between the Acropolis and Bozyertepe remained marine. Due to the ongoing seaward shift of the shoreline, a harbour on the western flank of the Acropolis hill is unlikely at this time. Immediately south of the Acropolis, two harbours were constructed: the local geomorphology was consolidated and transformed into a closed harbour basin by the erection of two breakwaters (Seeliger *et al.*, 2013). The water depth of the closed harbour basin was circa 2.5 m; sufficient for all common battle and merchant ship classes used by the Pergamenians at that time (Seeliger *et. al.*, 2017). Similar considerations also hold true for the area of the open harbour, including the presumed Hellenistic ship sheds where the water depth was circa 1.2 m (Pirson, 2010; Pint *et al.*, 2015; Seeliger *et al.*, 2017). As this area was essentially used to haul vessels into the ship sheds, the water was deep enough to operate ship sheds. In sum, both harbours were fully accessible and used for military and commercial purposes at this time (Pirson, 2004; Seeliger *et al.*, 2017; Pint *et al.*, 2015).

The eastern city district experienced a regression of the shoreline caused by denudation processes and human impacts (Shumilovskikh *et al.*, 2016). The coastal area was ideal for landing battleships while goods were most probably processed in the closed and the open harbours (Pirson 2011, 2014; Seeliger *et al.*, 2017). Torrential floods could have been a common temporary nuisance in the area, but nothing is known about this from the literature. Further south the shoreline leaves a narrow passage between the slopes of the Yuntdağ and the sea (Figs. 1, 2, 9). This underlines Elaia's strategic position: the city did not only serve as the main harbour of Pergamon, it was also a defensive stronghold, which secured the southern entrance to the inner realm of the lower Kaikos area (Seeliger *et al.*, 2013; Pirson, 2014; Figs. 1, 2). This topographic setting is comparable to that of Thermopylae in central Greece, where, in 480 BC, the legendary 300 Spartans fought bravely to withstand the far larger Persian army due to their strategic use of the landscape (Kraft *et al.*, 1987). Furthermore, it is reasonable to assume that a defence turret fortified the southern end of the city wall (Pirson, 2010). A turret would have necessitated a solid foundation when being constructed in a nearshore position; however, nothing of that kind was detected by coring. In Ela 65 (Figs. 2a, 9) only littoral sediments dating to the late Hellenistic to Roman periods were revealed.

**AD 500:** This scenario represents the time when Elaia was at or near the end of its prime. In several areas, the shoreline was close to its present position and sea level was only 0.4–0.6 m lower than today (Seeliger *et al.*, 2017). All corings present terrestrial sedimentation patterns for this period. The closed harbour basin had been abandoned and nearly silted up. The area of the former ship sheds was not accessible anymore (Seeliger *et al.*, 2013, 2017). Since the harbours were no longer usable, the people left the city. Most probably fearing pirate attacks, they moved to the landward settlement of *Püsküllü Tepeler* (Pirson, 2010; Seeliger *et al.*, 2014). As documented by pollen data, the natural vegetation grew back and many areas became woodland again (Shumilovskikh *et al.*, 2016). Saltworks were constructed, mostly built using spolia, about 2 km south of the city in the shallow bay. Salt was of great economic value and it was easy to harvest using a small workforce. Very shallow marine conditions and a very low energy wave climate in the bay favoured its use as a saltworks (Pirson, 2014; Seeliger *et al.*, 2014).

### *Elaia in the broader context of the Turkish Aegean coast*

Most ancient settlements in the Turkish Aegean region were situated along the coasts of enlarged marine embayments, formed during the Holocene marine transgression. Around 6000 BP, when sea-level rise slowed (Lambeck, 1996; Lambeck and Purcell, 2007), rivers became prominent morphogenetic agents, governing coastal changes by sediment supply, due to their prograding deltas. These settlements – for instance, Troy, Ainos, Ephesus, and

Miletos – faced numerous environmental challenges, such as the siltation of their harbours or the loss of their connection to the open sea (for location see Fig. 1b).

Troy is one of the most famous and best-studied examples (Figs. 1b, 10a; Kraft *et al.*, 1980, 2003). At the end of the Holocene marine transgression, the sea penetrated inland, about 10 km south of the later location of Troy. Deltaic progradation of the Scamander and Simois River followed by floodplain aggradation led to a northward shift of the shoreline. In the early Bronze Age (circa 3300 BC) Troy, as well as the Neolithic settlement of Kumtepe, were seaboard sites – comparable to the scene around 1500 BC in Elaia (Fig. 9) – protruding into a shallow marine embayment that still reached some kilometres further south and east of the settlements. At the time of the mythical Trojan War at the end of the late Bronze Age (most probably around 1200 BC) the delta front lay beyond but close to the settlement (Kraft *et al.*, 1980, 2003; Hertel, 2008; Brown, 2017). The present shoreline is situated some 4 km north of Troy and a strong longshore drift has hindered a further seaward progradation of the delta (Fig. 10a). Due to the long settlement history (3300 BC until AD 1200/1300 with interruptions, Troia I–Troia IX), the city hosted different harbour sites following the migrating shoreline. Based on a detailed summary of published work since the 1980s, Kayan (2014) suggests three possible harbour locations on the eastern slope of the Sigeion ridge (Fig. 10a). However, the southernmost possible location in the Yeniköy plain (YE in Fig. 10a) was already landlocked between 5000–3500 BP and a westward connection to the open Aegean by a canal or ditch crossing the Sigeion ridge is to be excluded in that case. Meanwhile, the silting up history of the Keşik plain (KE in Fig. 10a) is still open to discussion. While Kayan (2014) states a swamp at the time of the Trojan War, Kraft *et al.* (2003) assume a near-coastal shallow marine embayment in this area. In contrast to the Yeniköy plain, an opportunity to transport ships to the other side of the Sigeion ridge was proven for the Keşik plain. It was possible to transport ships from a protected harbour location in this area to the Aegean although the delta front had already prograded beyond this location. Finally, the northernmost area of the Kumtepe plain (KT in Fig. 10a) silted up last, most probably in late Hellenistic or early Roman Imperial times. Although Kayan (2014) does not advocate a harbour in this area, it would have been possible to land vessels at this location throughout the settlement period of Troy (Kraft *et al.*, 2003; Hertel, 2008; Kayan, 2014).

The ancient city of Ainos (Fig. 1b) is located close to the river mouth of the Hebros, which today debouches into the Aegean via an extensive deltaic floodplain of 180 km$^2$, between the Greek city of Alexandroupoli and the Turkish city Enez. Postglacial sea-level rise created a marine embayment which reached as far as the modern town of İpsala, i.e., 26 km inland.

Later, the delta front passed the city just after Roman Imperial times and may have caused a shift in the location of the city's harbours. Today, the city is situated about 2.5 km inland, separated from the Aegean by an extensive beach-barrier system (Alpar, 2001; Anthony *et al.*, 2014; Brückner *et al.*, 2015).

Further south, at ancient Ephesus (Fig. 1b) and its famous Artemision, sediment transported by the Küçük Menderes River led to a widespread siltation of the Küçük Menderes graben. The prograding delta caused a siltation of the harbours and the Ephesians were eventually forced to construct a "harbour channel" to maintain an access route to the sea after the delta front prograded beyond the city (e.g. Kraft *et al.*, 2007; Delile *et al.*, 2015; Ledger *et al.*, 2018).

Finally, the palaeoenvironmental model of Küçük Menderes graben can also be transposed to the Büyük Menderes graben, circa 50 km south. As the longest waterway flowing into the Turkish Aegean, the Büyük Menderes River led to the disconnection of ancient Miletos and Priene, situated on the southern flank of the Büyük Menderes graben, from the open sea and the demise of their harbours (e.g. Brückner *et al.,* 2006, 2013; Kazancı *et al.,* 2009).

In contrast, Fig. 10b presents the coastal configuration of the wider Elaia region. Unlike the above-mentioned settlements, Elaia is not situated on the inner part of the Kaikos- or Zeytindağ graben. The Bozyertepe ridge separates it from the Zeytindağ graben and therefore protects it from the fluvial sediments of the Kaikos. This is supported by the absence of fluvial sediments in the cores (unit 6). The siltation of the harbours of Elaia was therefore not as strong triggered by deltaic progradation as for the above mentioned examples, but also by slope wash of terrestrial material from the nearby Yuntdağ and Bozyertepe. As studies investigating the deltaic evolution of the Kaikos are lacking at present, it is speculative to further comment on this topic. Nevertheless, remains of a Roman-age bridge, just west of the Bozyertepe, documents that the delta front had already prograded beyond this location before this date. Based on corings, the evolution of the small island (I on Fig. 10b) was dated to post-15th century AD (Körfgen, 2014), showing that the most distal extension of the delta happened recently. As a result, because the influence of a major river delta is secondary, the harbour basins of Elaia were not massively affected by siltation which is borne out by the absence of dredging. Dredging is widely attested in other Mediterranean harbours such as Naples (Delile *et al.*, 2016), Portus (Salomon *et al.*, 2012), Tyre (Marriner and Morhange, 2006), Marseille (Morhange *et al.*, 2003) and Ephesus (Kraft *et al.*, 2007; Delile *et al.*, 2015). In addition, due to the short settlement period of Elaia (maximum 1000 years) – bracketed by natural conditions before and after it – the closed harbour basin constitutes a valuable geoarchive (Shumilovskikh *et al*., 2016).

## Conclusion

Around 1500 BC, the marine extension in the Bay of Elaia was at its maximum. The sea protruded circa 400 m inland in the northern and western areas; thus, the Acropolis was transformed into a peninsula. Due to the adjacent Yuntdağ Mountains, the extension of the sea to the east of Elaia was far less significant than in the western part. Siltation led to a gradual regression of the shoreline, mostly due to human activities during the ensuing centuries (Shumilovskikh *et al*., 2016).

During Hellenistic and Roman times, from ~300 BC onwards, three harbour areas were operational: the closed harbour, the open harbour, and the beach harbour. While the closed harbour was used for commercial and military purposes, the open harbour most likely housed the ship sheds with the battleships of the Pergamenians. The eastern city district with its beach harbour served as a place of temporary residence for foreign merchants, sailors, and soldiers (Pirson, 2010, 2014; Seeliger *et al*., 2017; Pint *et al*., 2015; Feuser *et al*., 2018). The siltation of the harbours contributed to the decline of the city in late Roman times led to its eventual abandonment (after AD 500). Human activities hugely influenced landscape changes. First of all, erosional processes became prominent in the densely populated and intensively used eastern part of the Bay of Elaia while these impacts were relatively minor in the western part, far from the settled area. Pint *et al*. (2015) have already demonstrated that the siltation of the open harbour area accelerated during the settlement period of Elaia. This may have resulted from the construction of the closed harbour basin and its breakwaters while impeding the bay's counterclockwise coastal cell, creating a sediment trap east of the closed harbour directly in front of the open harbour area (Figs. 2, 9).

While the population of Elaia shrank during Late Antiquity, the remaining inhabitants went to great lengths to construct the saltworks, which definitely had a strong influence on the environment and the sea currents in this area. Finally, in contrast to many other ancient settlements on the Turkish Aegean coast, Elaia was not significantly affected by siltation of a major river delta. As a consequence, no indications – neither sedimentological or literary – report dredging inside Elaia's different harbours. Due to the relatively short urban period of around 1000 years Elaia has a particular potential to study human-nature relations in the Hellenistic-Roman Imperial period, and the abandonment of a late antique city and the subsequent return to natural conditions (Shumilovskikh *et al*., 2016; Prison, in print).

## Acknowledgements

Financial support from the German Research Foundation is gratefully acknowledged (DFG ref. no. PI 740/1–3). Our research was part of the greater Elaia-Survey Project, headed by Felix Pirson, Director of the DAI Istanbul and excavation director of Pergamon. The Ministry of Culture and Tourism of the Republic of Turkey kindly granted the research permits. This work is a contribution to IGCP Project 639 *“Sea-Level Changes from Minutes to Millennia*”. Svenja Riedesel acknowledges financial support from an AberDoc-PhD scholarship (Aberystwyth University, UK). We acknowledge constructive comments by the editor of JQS Geoff Duller (Aberystwyth University, UK) and by Matteo Vacchi (University of Exeter, UK).

## References

Ad-Hoc-AG Boden. 2005. *Bodenkundliche Kartieranleitung*. Schweizerbart: Stuttgart. (in German)

Aksu AE, Piper DJW, Konuk T. 1987. Late Quaternary tectonic and sedimentary history of outer İzmir and Çandarlı Bays, Western Turkey. *Marine Geology* **76:** 89–104.

Alpar B. 2001. Plio-Quaternary history of the Turkish coastal zone of the Enez-Evros Delta: NE Aegean Sea. *Mediterranean Marine Science* **2(2):** 95–118.

Altunkaynak S, Yilmaz Y, 1998. The Mount Kozak magmatic complex. *Western Anatolia Journal of Volcanology and Geothermal Research* **85:** 211–231.

Ammerman AJ, Efstratiou N, Ntinou M *et al.* 2008. Finding the early Neolithic in Aegean Thrace: the use of cores. *Antiquity* **315:** 139–150.

Anthony EJ, Marriner N, Morhange C. 2014. Human influence and the changing geomorphology of Mediterranean deltas and coasts over the last 6000 years: from progradation to destruction phase? *Earth-Science Reviews* **139:** 336–361.

Bartz M, Klasen N, Zander A *et al.* 2015. Luminescence dating of ephemeral stream sediments around the Palaeolithic site of Ifri n'Ammar (Morocco). *Quaternary Geochronology* **30**: 460–465.

Bartz M, Rixhon G, Kehl M *et al.* 2017. Unravelling fluvial deposition and pedogenesis in ephemeral stream deposits in the vicinity of the prehistoric rock shelter of Ifri n'Ammar (NE Morocco) during the last 100 ka. *Catena* **152**: 115–134.

Başaran S. 2010. *Ainos (Enez)*, University İstanbul Press, İstanbul.

Benjamin J, Rovere A, Fontana A *et al.* 2017. Late Quaternary sea-level changes and early human societies in the central and eastern Mediterranean Basin: An interdisciplinary review. *Quaternary International* **449:** 29–57.

Blott SJ, Pye K. 2001. GRADISTAT: a grain size distribution and statistics package for the analysis of unconsolidated sediments. *Earth Surface Processes and Landforms* **26:** 1237–1248.

Bonaduce G, Ciampo G and Masoli M. 1975. Distribution of Ostracoda in the Adriatic Sea. *Pubblicazioni della Stazione zoologica di Napoli* **40** (Suppl.): 1–304.

Brown J. 2017. *Homeric Sites Around Troy,* Parrot Press, Canberra.

Brückner H. 1994. Das Mittelmeergebiet als Naturraum. In *Das Alte Rom,* Martin J (ed). Bertelsmann, München, 13–29.

Brückner H, Müllenhoff M, Gehrels R *et al.* 2006. From archipelago to floodplain - geographical and ecological changes in Miletus and its environs during the past six millennia (Western Anatolia, Turkey). *Zeitschrift für Geomorphologie N.F.* **142 (Suppl):** 63–83.

Brückner H, Urz R, Seeliger M. 2013. Geomorphological and geoarchaeological evidence for considerable landscape changes at the coasts of western Turkey during the Holocene. *Geopedology and Landscape Development Research Series* **1**: 81–104.

Brückner H, Schmidts T, Bücherl H *et al.* 2015. Die Häfen und ufernahen Befestigungen von Ainos - eine Zwischenbilanz. In *Häfen im ersten Millennium AD. Bauliche Konzepte, herrschaftliche und religiöse Einflüsse,* Schmidts T, Vučetić MM (eds). Verlag des Römisch-Germanischen Zentralmuseums, Mainz, 53–76.

Cartledge P. 2004. *Alexander the Great. The Hunt for a New Past,* Overlook Press, New York.

Cimerman F, Langer MR. 1991. *Mediterranean foraminifera*. Slovenska Akademija Znanosti in Umetnosti, Academia Scientarium et Artium Slovenca, Ljubljana.

Delile H, Blichert-Toft J, Goiran JP *et al.* 2015. Demise of a harbor: A geochemical chronicle from Ephesus. *Journal of Archaeological Science* **53:** 202–213.

Delile H, Goiran J-P, Blichert-Toft J *et al.* 2016. A geochemical and sedimentological perspective of the life cycle of Neapolis harbour (Naples, southern Italy). *Quaternary Science Reviews* **150:** 84–97.

Evelpidou N, Karkani A, Kampolis I *et al.* 2017. Late Holocene shorelines in east Attica (Greece). *Quaternary International* **436:** 1–7.

Ernst W. 1970. *Geochemical facies analysis,* Elsevier, Amsterdam, London, New York.

Feuser S, Pirson F, Seeliger M. 2018. The Harbour Zones of Elaia – the Maritime City of Pergamum. In *Harbours as objects of interdisciplinary research – Archaeology + History + Geosciences,* von Carnap-Bornheim C, Daim F, Ettel P, Warnke U (eds). Verlag des Römisch-Germanischen Zentralmuseums, Mainz, 91–103.

Flaux C, Marriner N, el-Assal M *et al.* 2017. Late Holocene erosion of the Canopic promontory (Nile Delta, Egypt). *Marine Geology* **385:** 56–67.

Folk RL, Ward WC. 1957. Brazos River bar: a study in the significance of grain size parameters. *Journal of Sedimentary Petrology* **27:** 3–26.

Frenzel P, Boomer I. 2005. The use of ostracods from marginal-marine, brackish waters as bioindicators of modern and Quaternary environmental change. *Palaeogeography, Palaeoclimatology, Palaeoecology* **225(1–4):** 68–92.

Giaime M, Morhange C, Ontiveros MAC *et al.* 2017. In search of Pollentia's southern harbour: Geoarchaeological evidence from the Bay of Alcúdia (Mallorca, Spain). *Palaeogeography, Palaeoclimatology, Palaeoecology* **466:** 184–201.

Goodman BN, Reinhardt E, Dey H *et al.* 2008. Evidence for Holocene marine transgression and shoreline progradation due to barrier development in Iskele, Bay of Izmir, Turkey. *Journal of Coastal Research* **24(5):** 1269–1280.

Goodman BN, Reinhardt EG, Dey HW *et al.* 2009. Multi-proxy geoarchaeological study redefines understanding of the paleocoastlines and ancient harbours of Liman Tepe (Iskele, Turkey). *Terra Nova* **21(2):** 97–104.

Hadler H, Kissas K, Koster B *et al.* 2013. Multiple Late-Holocene tsunami landfall in the eastern Gulf of Corinth recorded in the palaeotsunami geoarchive at Lechaion, harbour of ancient Corinth (Peloponnese, Greece). *Zeitschrift für Geomorphologie N.F.* **57(4) (Suppl):** 139–180.

Hansen E. 1971. *The Attalids of Pergamon*, Cornell University Press, Ithaca.

Hertel D. 2008. *Troia – Archäologie Geschichte Mythos*, C. H. Beck, München.

Horejs B. 2012. Çukuriçi Höyük. A Neolithic and Bronze Age Settlement in the Region of Ephesos. In *The Neolithic in Turkey. New Excavations & New Research*, Özdoğan M, Başgelen N, Kuniholm P (eds). Archaeology and Art Publications, İstanbul, 117–131.

Horejs B, Milić B, Ostmann F *et al.* 2015. The Aegean in the Early 7th Millennium BC: Maritime Networks and Colonization. *Journal of World Prehistory* **28(4):** 289–330.

Jeckelmann C. 1996. *Genese lokaler Thermalwasservorkommen in der Region Bergama/W-Türkei - Hydrochemie, Gas- und Isotopenanalysen zur Korrelation tiefer Grundwasserzirkulation und aktiver Tektonik*. PhD-Thesis, University of Zürich, Switzerland.

Joachim F, Langer M. 2008. *The 80 most common ostracods from the Bay of Fetoveia, Elba Island (Mediterranean Sea)*, University Bonn Press, Bonn.

Kayan I. 1999. Holocene stratigraphy and geomorphological evolution of the Aegean coastal plains of Anatolia. *Quaternary Science Reviews* **18:** 541–548.

Kayan I. 2014. Geoarchaeological Research at Troia and its Environs. In *Troia 1987–2012: Grabungen und Forschungen I – Forschungsgeschichte, Methoden und Landschaft*, Pernicka E, Rose CB, Jablonka P (eds), Verlag Dr. Rudolf-Habelt, Bonn, 694–731.

Kazancı N, Dündar S, Alçiçek MC *et al.* 2009. Quaternary deposits of the Büyük Menderes Graben in western Anatolia, Turkey: Implications for river capture and the longest Holocene estuary in the Aegean Sea. *Marine Geology* **264:** 165–176.

Khan NS, Ashe E, Shaw TA *et al.* 2015. Holocene relative sea-level changes from near-, intermediate-, and far-field locations. *Current Climate Change Reports* **1(4):** 247–262.

Körfgen K. 2014. *Die Analyse des Bohrkerns ELA 84 – Ein Beitrag zur sedimentologischen Entwicklung der Bucht von Elaia, Westtürkei*. Bachelor's-Thesis, University of Cologne, Germany.

Kraft JC, Aschenbrenner SE, Rapp G Jr. 1977. Paleogeographic reconstructions of coastal Aegean archaeological sites. *Science* **195:** 941–947.

Kraft JC, Kayan I, Erol O. 1980. Geomorphic reconstructions in the environs of ancient Troy. *Science* **209:** 776–782.

Kraft JC, Rapp G, Szemler GJ *et al.* 1987. The pass at Thermopylae, Greece. *Journal of Field Archaeology* **14:** 181–198.

Kraft JC, Kayan I, Luce JV. 2003. Harbor areas at ancient Troy: sedimentology and geomorphology complement Homer's Iliad. *Geology* **31(2):** 163–166.

Kraft JC, Brückner H, Kayan I *et al.* 2007. The geographies of ancient Ephesus and the Artemision in Anatolia. *Geoarchaeology* **22:** 121–149.

Lambeck K. 1996. Sea-level change and shore-line evolution in Aegean Greece since Upper Palaeolithic time. *Antiquity* **70**: 588–611.

Lambeck K, Purcell A. 2007. Palaeogeographic reconstructions of the Aegean for the past 20,000 years: Was Atlantis on Athens doorstep? In *The Atlantis Hypothesis: Searching for a Lost Land*, Papamarinopoulos SP (ed). Heliotopos Publications, Santorini, 241–257.

Ledger ML, Stock F, Schwaiger H *et al.* 2018. Intestinal parasites from public and private latrines and the harbour canal in Roman Period Ephesus, Turkey (1st c. BCE to 6th c. CE). *Journal of Archaeological Science: Reports* **21**: 289–297.

Lubos C, Dreibrodt S, Bahr A. 2016. Analysing spatio-temporal patterns of archaeological soils and sediments by comparing pXRF and different ICP-OES extraction methods. *Journal of Archaeological Science: Reports* **9**: 44–53.

Marriner N, Morhange C. 2006. Geoarchaeological evidence for dredging in Tyre's ancient harbour, Levant. *Quaternary Research* **65:** 164–171.

Marriner N, Morhange C, Kaniewski D *et al.* 2014. Ancient harbour infrastructure in the Levant: tracking the birth and rise of new forms of anthropogenic pressure. *Scientific Reports* **4:** 5554.

Meriç E, Avşar N, Bergin F. 2004. Benthic foraminifera of eastern Aegean Sea (Turkey); systematics and autecology. *Turkish Marine Research Foundation* **18:** 1–306.

Morhange C, Giaime M, Marriner N *et al.* 2016. Geoarchaeological evolution of Tel Akko's ancient harbour (Israel). *Journal of Archaeological Science: Reports* **7:** 71–81.

Morhange C, Blanc F, Bourcier M *et al.* 2003. Bio-sedimentology of the late Holocene deposits of the ancient harbour of Marseilles (Southern France, Mediterranean Sea). *The Holocene* **13:** 593–604.

Murray JW, 2006. *Ecology and Applications of Benthic Foraminifera*, Cambridge University Press, New York.

Murray-Wallace CV, Woodroffe CD. 2014. *Quaternary Sea-Level Changes: A Global Perspective,* Cambridge University Press, Cambridge.

Özbek O. 2010. Hamaylıtarla reconsidered: A Neolithic site and its environmental setting in southern Thrace. *Anatolia Antiqua* **18(1):** 1–21.

Pennington BT, Sturt F, Wilson P *et al.* 2017. The fluvial evolution of the Holocene Nile Delta. *Quaternary Science Reviews* **170:** 212–231.

Pint A, Seeliger M, Frenzel P *et al.* 2015. The environs of Elaia's ancient open harbour - a reconstruction based on microfaunal evidence. *Journal of Archaeological Science* **54:** 340–355.

Pirson F. 2004. Elaia, der maritime Satellit Pergamons. *Istanbuler Mitteilungen* **54:** 197–213.

Pirson F. 2007. Elaia. *Archäologischer Anzeiger* **2007(2):** 47–58.

Pirson F. 2008. Das Territorium der hellenistischen Residenzstadt Pergamon – Herrschaftlicher Anspruch als raumbezogene Strategie. In *Räume der Stadt - Von der Antike bis heute,* Jöchner C (ed). Reimer: Berlin; 27–50.

Pirson F. 2010. Survey. *Archäologischer Anzeiger* **2010(2):** 195–201.

Pirson F. 2011. Elaia. *Archäologischer Anzeiger* **2011(2):** 166–174.

Pirson F. 2014. Elaia, der (maritime) Satellit Pergamons. In *Harbour Cities in the Eastern Mediterranean from Antiquity to the Byzantine Period,* Ladstätter S, Pirson F, Schmidts T (eds), Ege Yayinlari, İstanbul, 339–356.

Pirson F. (in print). Nature, Religion, and Urban Aesthetics in Ancient Pergamon and its Micro-region. Some Thoughts on the Potential of an `Ecological Turn´ for Classical Archaeology (and beyond). In *Ecologies, Aesthetics, and Histories of Art*, Baader H, Ray S, Wolf G, (eds.), de Gruyter, Berlin.Pirson F. Scholl A. 2015. *Pergamon. A Hellenistic Capital in Anatolia,* Ege Yayinlari, İstanbul.

Radt W. 2016. *Pergamon – Geschichte und Bauten einer antiken Metropole*. Primus Verlag: Darmstadt.

Reimer PJ, Bard E, Bayliss A *et al.* 2013. IntCal13 and MARINE13 radiocarbon age calibration curves 0-50000 years calBP. *Radiocarbon* **55(4):** 1869–1887.

Salomon F, Delile H, Goiran J-P *et al.* 2012. The Canale di Comunicazione Traverso in Portus: The Roman sea harbour under river influence (Tiber delta, Italy). *Géomorphologie* **1:** 75–90.

Seeliger M, Bartz M, Erkul E *et al.* 2013. Taken from the sea, reclaimed by the sea: The fate of the closed harbour of Elaia, the maritime satellite city of Pergamum (Turkey). *Quaternary International* **312:** 70–83.

Seeliger M, Brill D, Feuser S *et al.* 2014. The purpose and age of underwater walls in the Bay of Elaia of western Turkey: A multidisciplinary approach. *Gearchaeology* **29:** 138–155.

Seeliger M, Pint A, Frenzel P *et al.* 2017. Foraminifera as markers of Holocene sea-level fluctuations and water depths of ancient harbours – A case study from the Bay of Elaia (W Turkey). *Palaeogeography, Palaeoclimatology, Palaeoecology* **482:** 17–29.

Seeliger M, Pint A, Frenzel P *et al.* 2018. Using a Multi-Proxy Approach to Detect and Date a Buried part of the Hellenistic City Wall of Ainos (NW Turkey). *Geosciences* **8(10)**, 357.

Shumilovskikh LS, Seeliger M, Feuser S *et al.* 2016. The harbour of Elaia: A palynological archive for human/environmental interactions during the last 7500 years. *Quaternary Science Reviews* **149:** 167–187.

Siani G, Paterne M, Arnold M *et al.* 2000. Radiocarbon reservoir ages in the Mediterranean Sea and Black Sea. *Radiocarbon* **42:** 271–280.

Stock F, Ehlers L, Horejs B *et al*. 2015. Neolithic settlement sites in Western Turkey - palaeogeographic studies at Çukuriçi Höyük and Arvalya Höyük. *Journal of Archaeological Science: Reports* **4:** 565–577.

Strabo. 2005. *Geographica*. Translation and comments by Albert Forbiger, Marix Verlag, Wiesbaden.

Vacchi M, Rovere A, Chatzipetros A *et al.* 2014. An updated database of Holocene relative sea level changes in NE Aegean Sea. *Quaternary International* **328-329:** 301–310.

Vacchi M, Marriner N, Morhange C *et al.* 2016a. Multiproxy assessment of Holocene relative sea-level changes in the western Mediterranean: sea-level variability and improvements in the definition of the isostatic signal. *Earth-Science Reviews* **155:** 172–197.

Vacchi M, De Falco G, Simeone S *et al.* 2016b. Biogeomorphology of the Mediterranean *Posidonia oceanica* seagrass meadows. *Earth Surface Processes and Landforms* **42:** 42–54.

Vita-Finzi C. 1969. Late Quaternary continental deposits of central and western Turkey. *Man New Series* **4(4):** 605–619.

Vött A, Bareth G, Brückner H *et al.* 2011. Olympia’s harbour site Pheia (Elis, Western Peloponnese, Greece) destroyed by tsunami impact. *Die Erde* **142(3):** 259–288.

Yoo J, Rohli RV. 2016. Global distribution of Köppen–Geiger climate types during the Last Glacial Maximum, Mid-Holocene, and present. *Palaeogeography, Palaeoclimatology, Palaeoecology* **446:** 326–337.

Zimmermann M. 2011. *Pergamon: Geschichte, Kultur, Archäologie*, C.H. Beck, München.

## Caption of Figures and Tables

**Figure 1.** The study area on the Aegean coast of Turkey. (a) Structural map and surrounding mountain ranges. Bergama and Zeytindağ grabens are marked in yellow. The study area of Elaia (Fig. 2a) is denoted in pale red. Source: Altunkaynak and Yilmaz (1998), substantially modified, with locations mentioned in the text. Insert: (b) General map of the Turkish Aegean coast with the position of the study area (Fig. 1a) and further ancient settlements mentioned in this paper. Source: Radt (2016), substantially modified. (c) Timeline of the historical periods, linked with the period of Elaia's prime (based on: Pirson and Scholl, 2015; Radt, 2016).

**Figure 2.** Locations of selected vibracores taken in the Bay of Elaia. (a) Locations of coring transects A–A', B–B', D–D', E–E' and F–F', "C" (coring Ela 58), and of the elevation profile XYZ shown in Fig. 2c. (b) Panoramic view of the study area (UAV image; taken on 01 September 2015 by A. Bolten) with the location of the harbour areas. (c) Elevation profile XYZ (based on Google Earth Pro; 21 July 2018). The enhanced relief energy of the eastern part in contrast to the western area of the Bay of Elaia is clearly evident.

**Figure 3.** Sediment core Ela 57 with geochemical and sedimentological parameters (a, b, c). (d) Interpretation of sedimentary units and dating results.

**Figure 4.** Sedimentary units of core Ela 57, based on microfauna. Relative abundance of ostracods and foraminifers is given semi-quantitatively.

**Figure 5.** Sediment core Ela 12 with geochemical and sedimentological parameters (a, b, c). (d) Interpretation of sedimentary units and dating result.

**Figure 6.** Sedimentary units of core Ela 12, based on microfauna. Relative abundance of ostracods and foraminifers is given semi-quantitatively.

**Figure 7.** Microfaunal, granulometric, and geochemical characteristics of the sedimentary units of the corings in the Bay of Elaia. Because these characteristics are dependant on regional factors (bedrock, weathering conditions etc.) care should be exercised before transposing these data to other study areas.

**Figure 8.** Synopsis of the coring transects (a) A–A', (b) B–B', (d) D–D', (e) E–E', and (f) F–F', as well as (c) (Ela 58); (g) legend; (h) locations of corings and transects.

**Figure 9.** Coastline changes in the Bay of Elaia in time slices: 1500 BC, 300 BC and AD 500. The scenarios are based on the results of this paper.

**Figure 10.** Comparison of the palaeoenvironmental evolution of Troy and Elaia. (a) The area of ancient Troy in Roman times. It clearly shows the influence of the Simois and Scamander Rivers on the surroundings of Troy, especially with regards to the coastline scenarios for 3300 BC (Late Neolithic/Early Bronze Age), 1300 BC (Iliad/Trojan War) and Roman times (based on Kraft *et al.*, 2003; abbreviations: KT=Kum-Tepe plain, KE=Keşik plain, YE=Yeniköy plain). (b) Present coastline configuration of the Bay of Elaia and the southernmost part of the Kaikos River added by assumed former coastlines of the Kaikos Delta. It becomes evident that the prograding delta of the Kaikos River did not influence the Bay of Elaia due to the shielding effect of the Bozyertepe ridge (personal compilation based on a QuickBird 2 satellite image, acquired: 2 April 2006).

**Table 1:** Radiocarbon data sheet. $^{14}$C-AMS dating was carried out at the Centre for Applied Isotope Studies (CAIS) of the University of Georgia in Athens, USA (lab code: UGAMS) and the $^{14}$Chrono Centre for Climate, the Environment, and Chronology, Queen's University Belfast, UK (lab code: UBA). All ages were calibrated with the IntCal13 or MARINE13 calibration curves depending on the samples $\delta^{13}$C using the recent Calib 7.1 software (Reimer *et al.*, 2013). A marine reservoir effect of

390±85 years and a ΔR of 35±70 years (Siani *et al.*, 2000) was applied. The calibrated ages are presented in calendar years BC/AD and years BP with 2σ confidence interval.

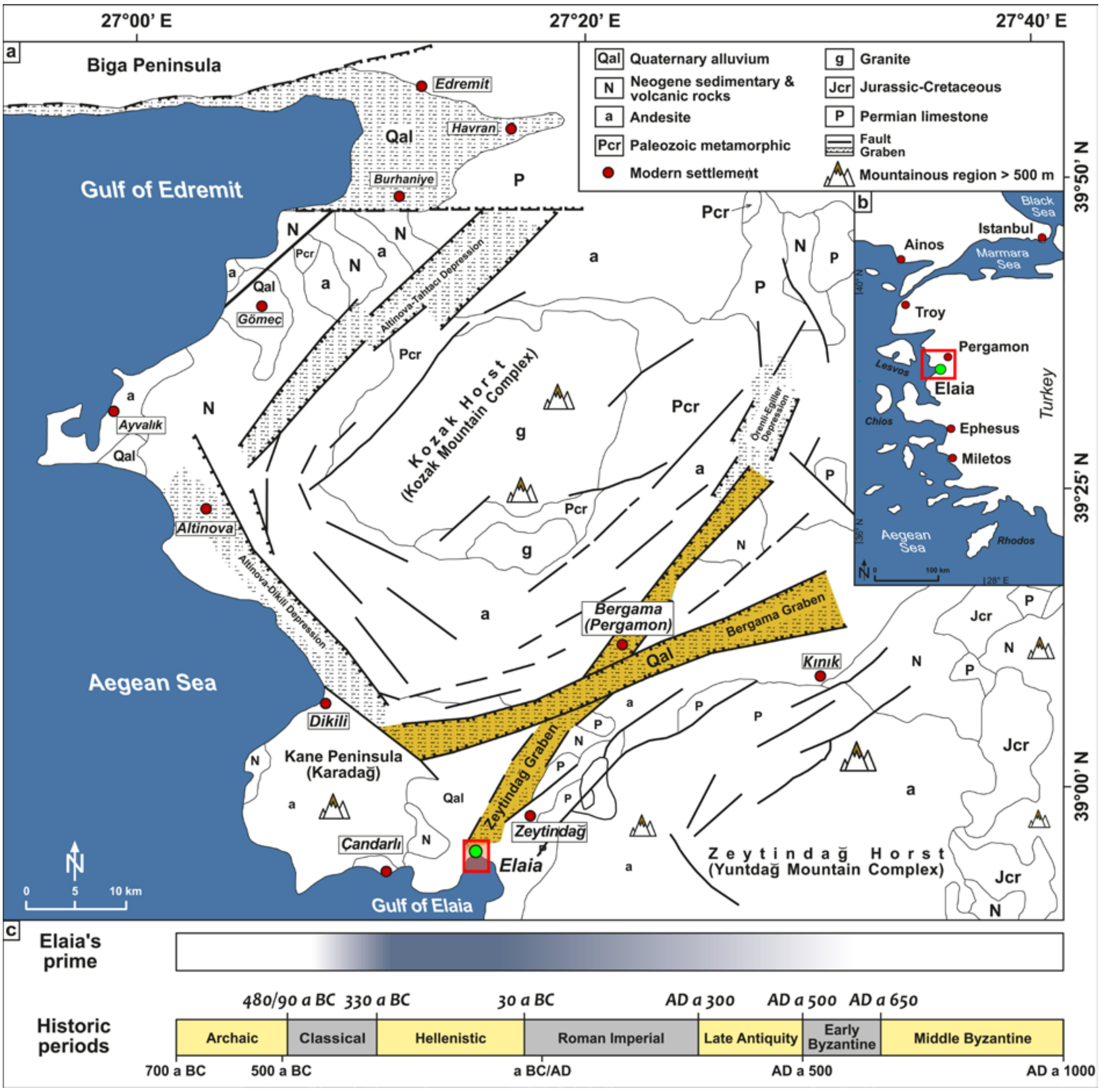
27°00' E
27°20' E
27°40' E
39°50' N
39°25' N
39°00' N
a
Biga Peninsula
Gulf of Edremit
Edremit
Havran
Burhaniye
Gömeç
Ayvalık
Altinova
Dikili
Çandarlı
Zeytindağ
Bergama (Pergamon)
Kınık
Elaia
Gulf of Elaia
Aegean Sea
Kane Peninsula (Karadağ)
Kozak Horst (Kozak Mountain Complex)
Zeytindağ Horst (Yuntdağ Mountain Complex)
Altinova-Tahtacı Depression
Altinova-Dikili Depression
Ören-Eğiller Depression
Bergama Graben
Zeytindağ Graben
Qal Quaternary alluvium
N Neogene sedimentary & volcanic rocks
a Andesite
Pcr Paleozoic metamorphic
Modern settlement
g Granite
Jcr Jurassic-Cretaceous
P Permian limestone
Fault
Graben
Mountainous region > 500 m
0 5 10 km
b
Black Sea
Istanbul
Marmara Sea
Ainos
Troy
Pergamon
Lesvos
Elaia
Chios
Ephesus
Miletos
Turkey
Aegean Sea
Rhodos
40° N
36° N
28° E
0 100 km
c
Elaia's prime
Historic periods
480/90 a BC
330 a BC
30 a BC
AD a 300
AD a 500
AD a 650
Archaic
Classical
Hellenistic
Roman Imperial
Late Antiquity
Early Byzantine
Middle Byzantine
700 a BC
500 a BC
a BC/AD
AD a 500
AD a 1000

Fig. 1.

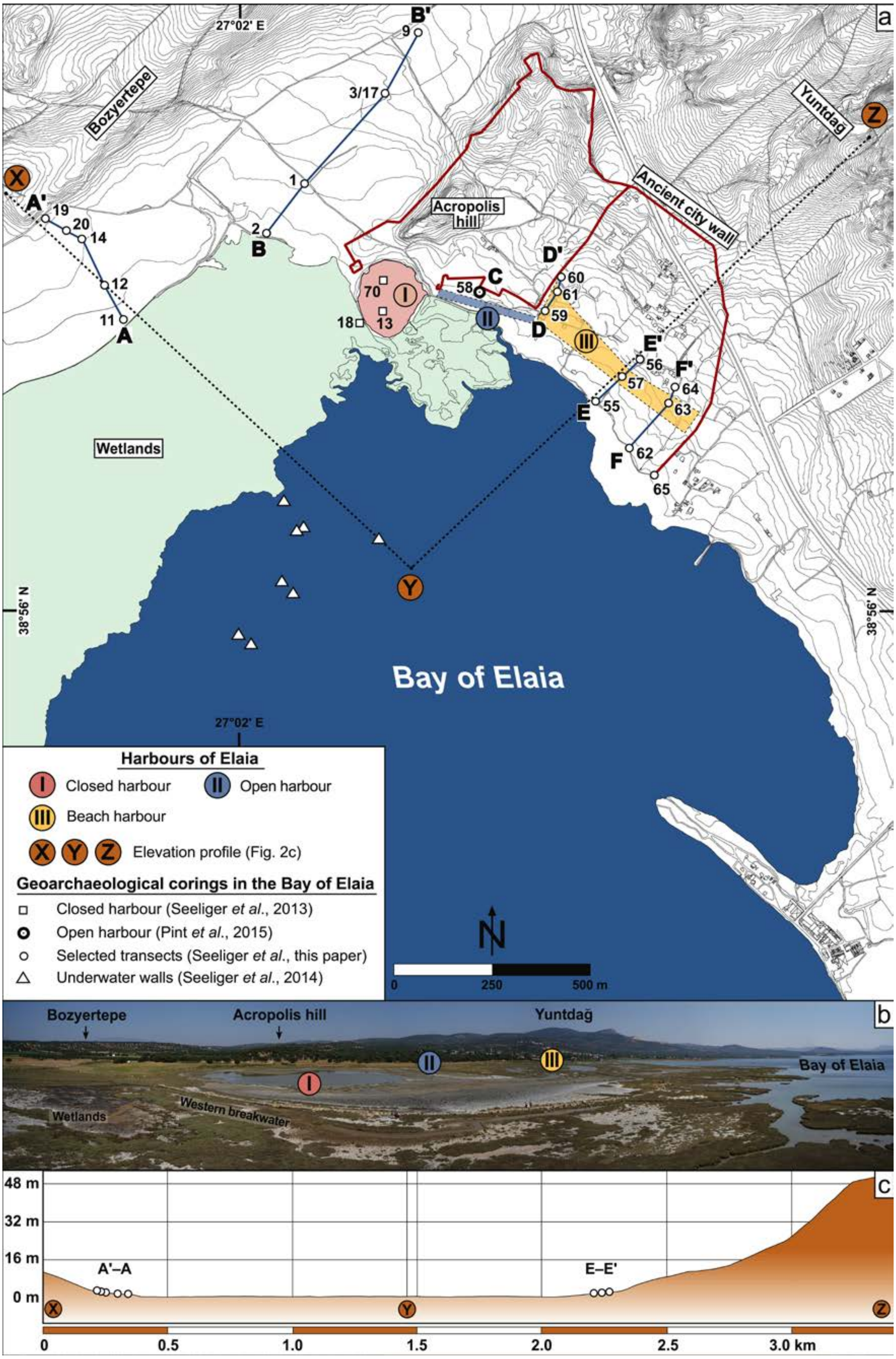
a
27°02' E
B'
9
3/17
1
2
B
Bozyertepe
X
A'
19
20
14
12
11
A
Acropolis hill
70
I
18
13
58
C
II
D'
60
61
59
D
III
E'
56
57
55
E
F'
64
63
62
F
65
Ancient city wall
Yuntdağ
Z
Wetlands
Y
38°56' N
Bay of Elaia
Harbours of Elaia
I Closed harbour
II Open harbour
III Beach harbour
X Y Z Elevation profile (Fig. 2c)
Geoarchaeological corings in the Bay of Elaia
□ Closed harbour (Seeliger et al., 2013)
Open harbour (Pint et al., 2015)
○ Selected transects (Seeliger et al., this paper)
△ Underwater walls (Seeliger et al., 2014)
N
0
250
500 m
b
Bozyertepe
Acropolis hill
Yuntdağ
Bay of Elaia
Wetlands
Western breakwater
c
48 m
32 m
16 m
0 m
A'–A
E–E'
0
0.5
1.0
1.5
2.0
2.5
3.0 km

**Fig. 2.**

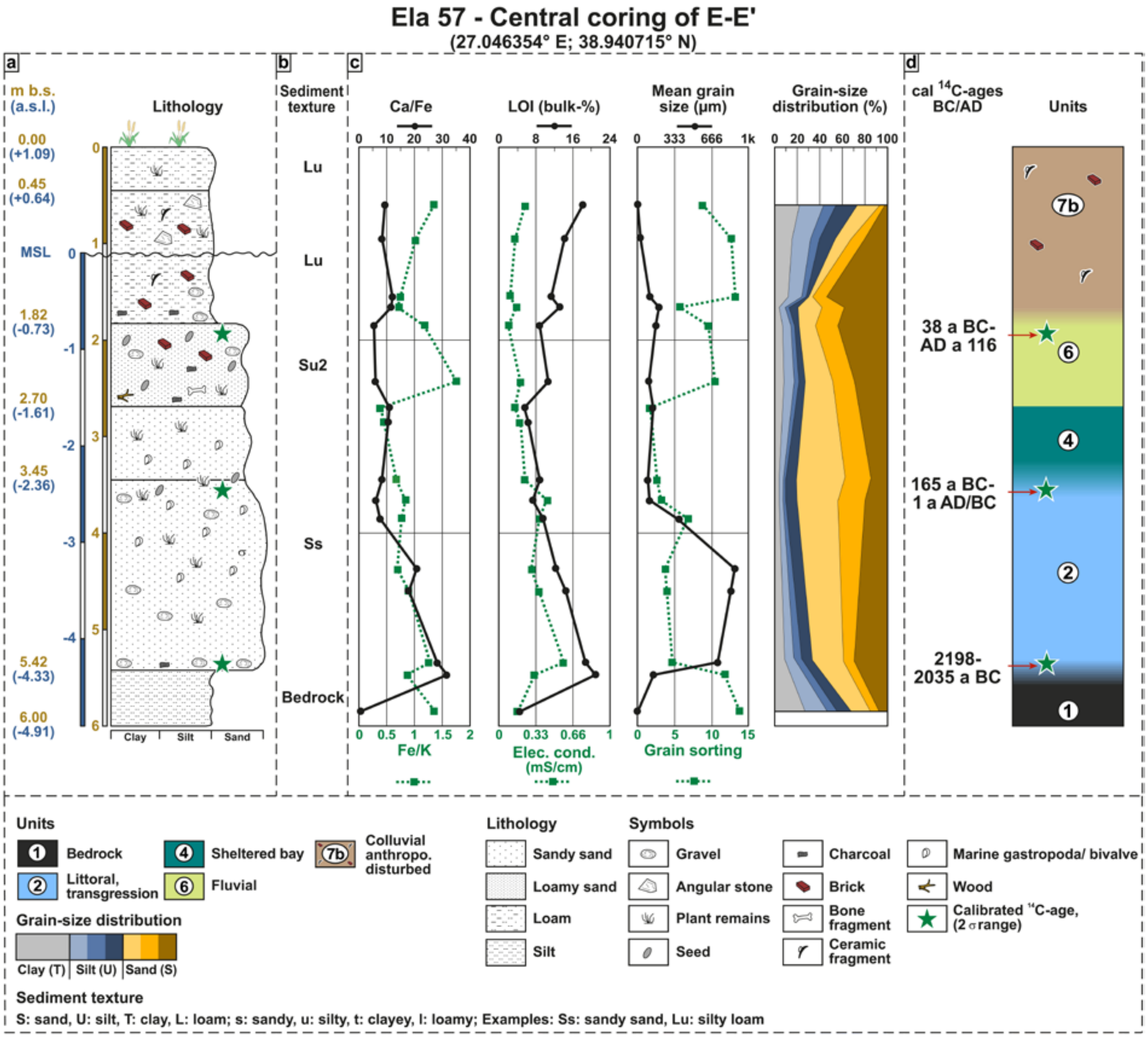
Ela 57 - Central coring of E-E'
(27.046354° E; 38.940715° N)
a
m b.s.
(a.s.l.)
Lithology
0.00
(+1.09)
0.45
(+0.64)
MSL
1.82
(-0.73)
2.70
(-1.61)
3.45
(-2.36)
5.42
(-4.33)
6.00
(-4.91)
0
-1
-2
-3
-4
0
1
2
3
4
5
6
Clay
Silt
Sand
b
Sediment texture
Lu
Lu
Su2
Ss
Bedrock
c
Ca/Fe
0
10
20
30
40
LOI (bulk-%)
0
8
16
24
Mean grain size (µm)
0
333
666
1k
Grain-size distribution (%)
0
20
40
60
80
100
0
0.5
1
1.5
2
Fe/K
0
0.33
0.66
1
Elec. cond. (mS/cm)
0
5
10
15
Grain sorting
d
cal $^{14}$C-ages BC/AD
Units
38 a BC-
AD a 116
165 a BC-
1 a AD/BC
2198-
2035 a BC
7b
6
4
2
1
Units
1 Bedrock
2 Littoral, transgression
4 Sheltered bay
6 Fluvial
7b Colluvial anthropo. disturbed
Grain-size distribution
Clay (T)
Silt (U)
Sand (S)
Lithology
Sandy sand
Loamy sand
Loam
Silt
Symbols
Gravel
Angular stone
Plant remains
Seed
Charcoal
Brick
Bone fragment
Ceramic fragment
Marine gastropoda/ bivalve
Wood
Calibrated $^{14}$C-age, (2 σ range)
Sediment texture
S: sand, U: silt, T: clay, L: loam; s: sandy, u: silty, t: clayey, l: loamy; Examples: Ss: sandy sand, Lu: silty loam

Fig. 3.

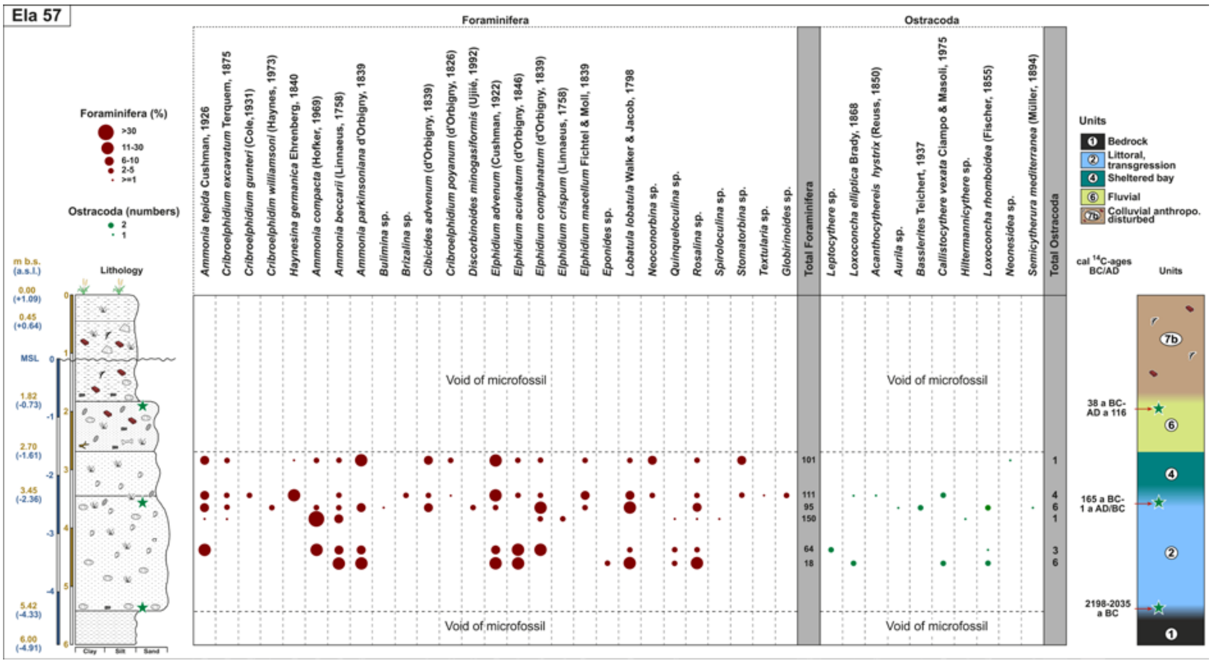
Ela 57
Foraminifera (%)
>30
11-30
6-10
2-5
>=1
Ostracoda (numbers)
2
1
m b.s.
(a.s.l.)
Lithology
0.00
(+1.09)
0.45
(+0.64)
MSL
1.82
(-0.73)
2.70
(-1.61)
3.45
(-2.36)
5.42
(-4.33)
6.00
(-4.91)
0
-1
-2
-3
-4
0
1
2
3
4
5
6
Clay
Silt
Sand
Foraminifera
Ammonia tepida Cushman, 1926
Cribroelphidium excavatum Terquem, 1875
Cribroelphidium gunteri (Cole,1931)
Cribroelphidim williamsoni (Haynes, 1973)
Haynesina germanica Ehrenberg, 1840
Ammonia compacta (Hofker, 1969)
Ammonia beccarii (Linnaeus, 1758)
Ammonia parkinsoniana d'Orbigny, 1839
Bulimina sp.
Brizalina sp.
Cibicides advenum (d'Orbigny, 1839)
Cribroelphidium poyanum (d'Orbigny, 1826)
Discorbinoides minogasiformis (Ujiié, 1992)
Elphidium advenum (Cushman, 1922)
Elphidium aculeatum (d'Orbigny, 1846)
Elphidium complanatum (d'Orbigny, 1839)
Elphidium crispum (Linnaeus, 1758)
Elphidium macellum Fichtel & Moll, 1839
Eponides sp.
Lobatula lobatula Walker & Jacob, 1798
Neoconorbina sp.
Quinqueloculina sp.
Rosalina sp.
Spiroloculina sp.
Stomatorbina sp.
Textularia sp.
Globirinoides sp.
Total Foraminifera
Ostracoda
Leptocythere sp.
Loxoconcha elliptica Brady, 1868
Acanthocythereis hystrix (Reuss, 1850)
Aurila sp.
Bassleriites Teichert, 1937
Callistocythere vexata Ciampo & Masoli, 1975
Hiltermannicythere sp.
Loxoconcha rhomboidea (Fischer, 1855)
Neonesidea sp.
Semicytherura mediterranea (Müller, 1894)
Total Ostracoda
Void of microfossil
Void of microfossil
Void of microfossil
Void of microfossil
101
111
95
150
64
18
1
4
6
1
3
6
Units
1 Bedrock
2 Littoral, transgression
4 Sheltered bay
6 Fluvial
7b Colluvial anthropo. disturbed
cal $^{14}$C-ages BC/AD
Units
38 a BC-AD a 116
165 a BC-1 a AD/BC
2198-2035 a BC
7b
6
4
2
1

**Fig. 4.**

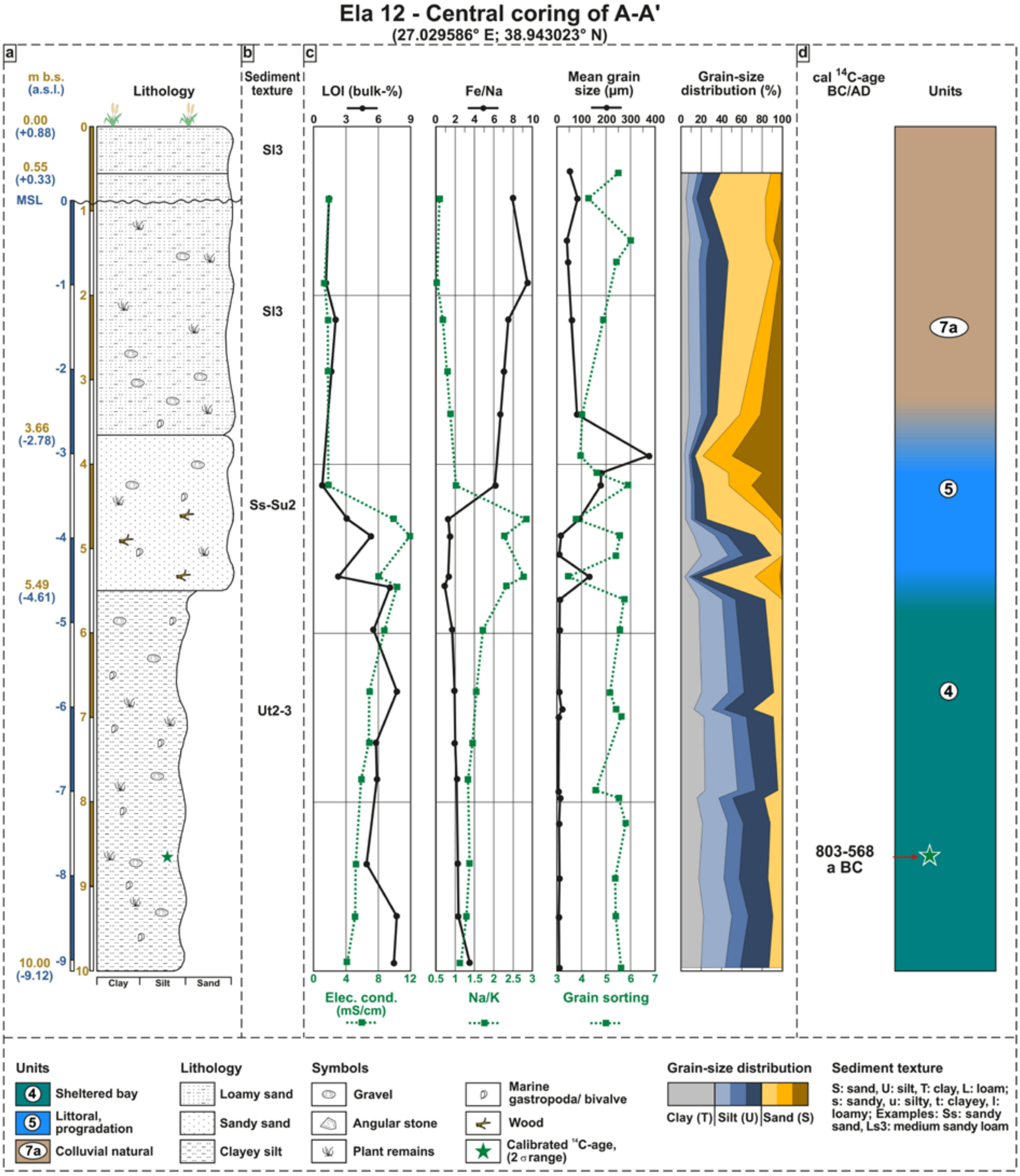
Ela 12 - Central coring of A-A'
(27.029586° E; 38.943023° N)
a
m b.s.
(a.s.l.)
Lithology
0.00
(+0.88)
0.55
(+0.33)
MSL
3.66
(-2.78)
5.49
(-4.61)
10.00
(-9.12)
Clay
Silt
Sand
b
Sediment texture
Sl3
Sl3
Ss-Su2
Ut2-3
c
LOI (bulk-%)
Fe/Na
Mean grain size (µm)
Grain-size distribution (%)
Elec. cond. (mS/cm)
Na/K
Grain sorting
d
cal $^{14}$C-age BC/AD
Units
7a
5
4
803-568 a BC
Units
4 Sheltered bay
5 Littoral, progradation
7a Colluvial natural
Lithology
Loamy sand
Sandy sand
Clayey silt
Symbols
Gravel
Angular stone
Plant remains
Marine gastropoda/ bivalve
Wood
Calibrated $^{14}$C-age, (2 σ range)
Grain-size distribution
Clay (T)
Silt (U)
Sand (S)
Sediment texture
S: sand, U: silt, T: clay, L: loam; s: sandy, u: silty, t: clayey, l: loamy; Examples: Ss: sandy sand, Ls3: medium sandy loam

**Fig. 5.**

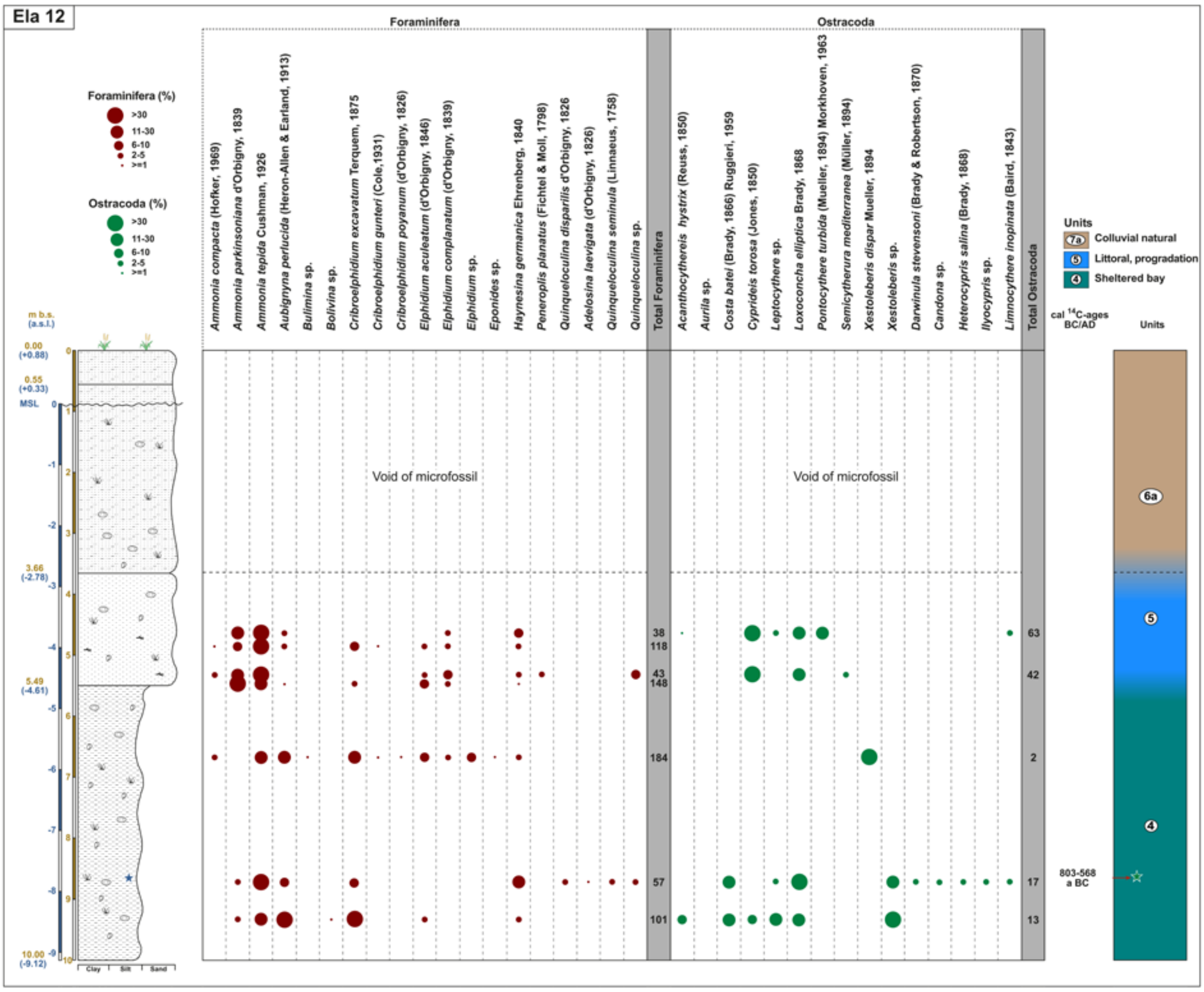
Ela 12
Foraminifera (%)
>30
11-30
6-10
2-5
>=1
Ostracoda (%)
>30
11-30
6-10
2-5
>=1
m b.s.
(a.s.l.)
0.00
(+0.88)
0.55
(+0.33)
MSL
3.66
(-2.78)
5.49
(-4.61)
10.00
(-9.12)
Clay
Silt
Sand
Foraminifera
Ammonia compacta (Hofker, 1969)
Ammonia parkinsoniana d'Orbigny, 1839
Ammonia tepida Cushman, 1926
Aubignyna perlucida (Heron-Allen & Earland, 1913)
Bulimina sp.
Bolivina sp.
Cribroelphidium excavatum Terquem, 1875
Cribroelphidium gunteri (Cole,1931)
Cribroelphidium poyanum (d'Orbigny, 1826)
Elphidium aculeatum (d'Orbigny, 1846)
Elphidium complanatum (d'Orbigny, 1839)
Elphidium sp.
Eponides sp.
Haynesina germanica Ehrenberg, 1840
Peneroplis planatus (Fichtel & Moll, 1798)
Quinqueloculina disparilis d'Orbigny, 1826
Adelosina laevigata (d'Orbigny, 1826)
Quinqueloculina seminula (Linnaeus, 1758)
Quinqueloculina sp.
Total Foraminifera
Ostracoda
Acanthocythereis hystrix (Reuss, 1850)
Aurila sp.
Costa batei (Brady, 1866) Ruggieri, 1959
Cyprideis torosa (Jones, 1850)
Leptocythere sp.
Loxoconcha elliptica Brady, 1868
Pontocythere turbida (Mueller, 1894) Morkhoven, 1963
Semicytherura mediterranea (Müller, 1894)
Xestoleberis dispar Mueller, 1894
Xestoleberis sp.
Darwinula stevensoni (Brady & Robertson, 1870)
Candona sp.
Heterocypris salina (Brady, 1868)
Ilyocypris sp.
Limnocythere inopinata (Baird, 1843)
Total Ostracoda
Void of microfossil
Void of microfossil
38
118
43
148
184
57
101
63
42
2
17
13
Units
7a Colluvial natural
5 Littoral, progradation
4 Sheltered bay
cal $^{14}$C-ages BC/AD
Units
6a
5
4
803-568 a BC

**Fig. 6.**

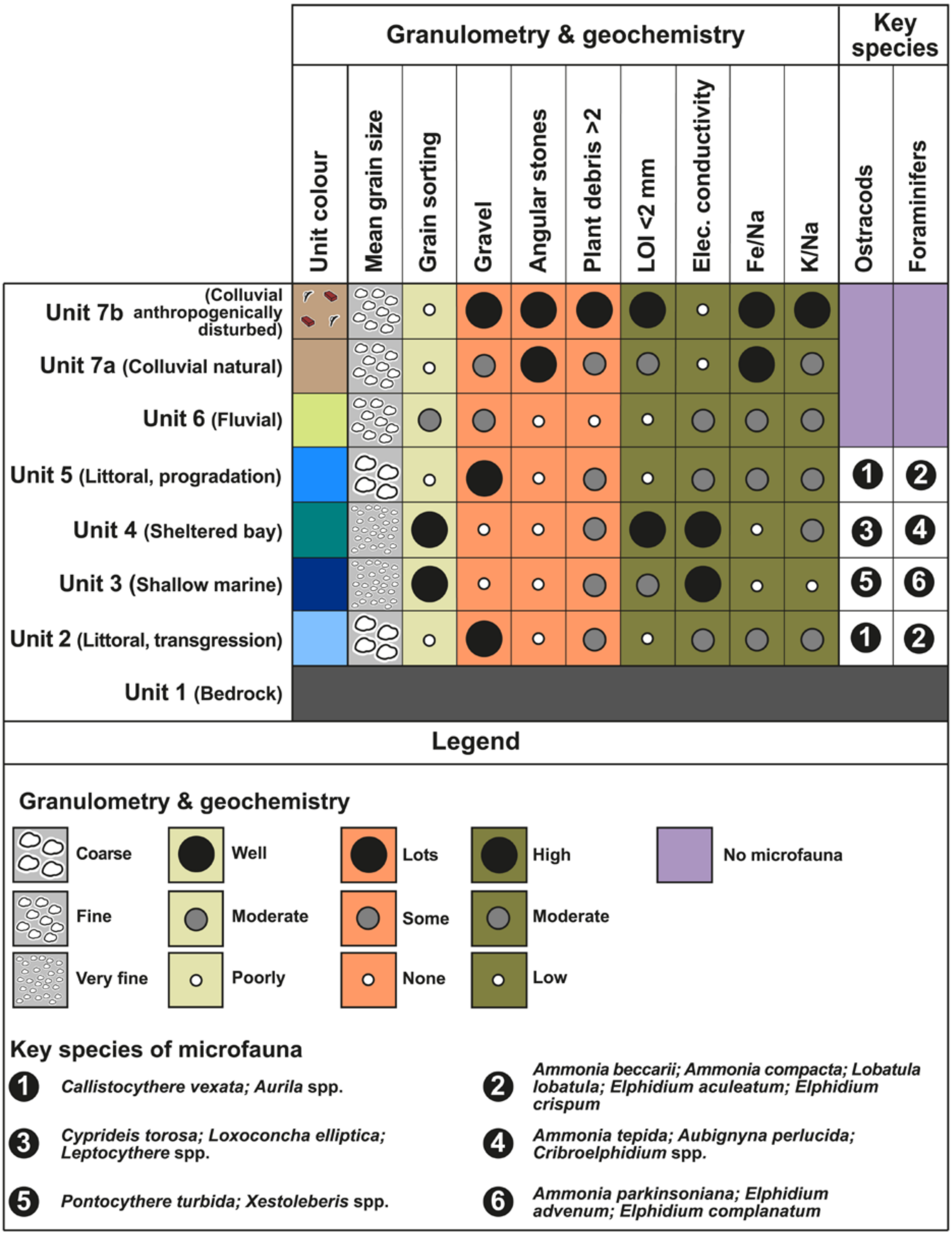

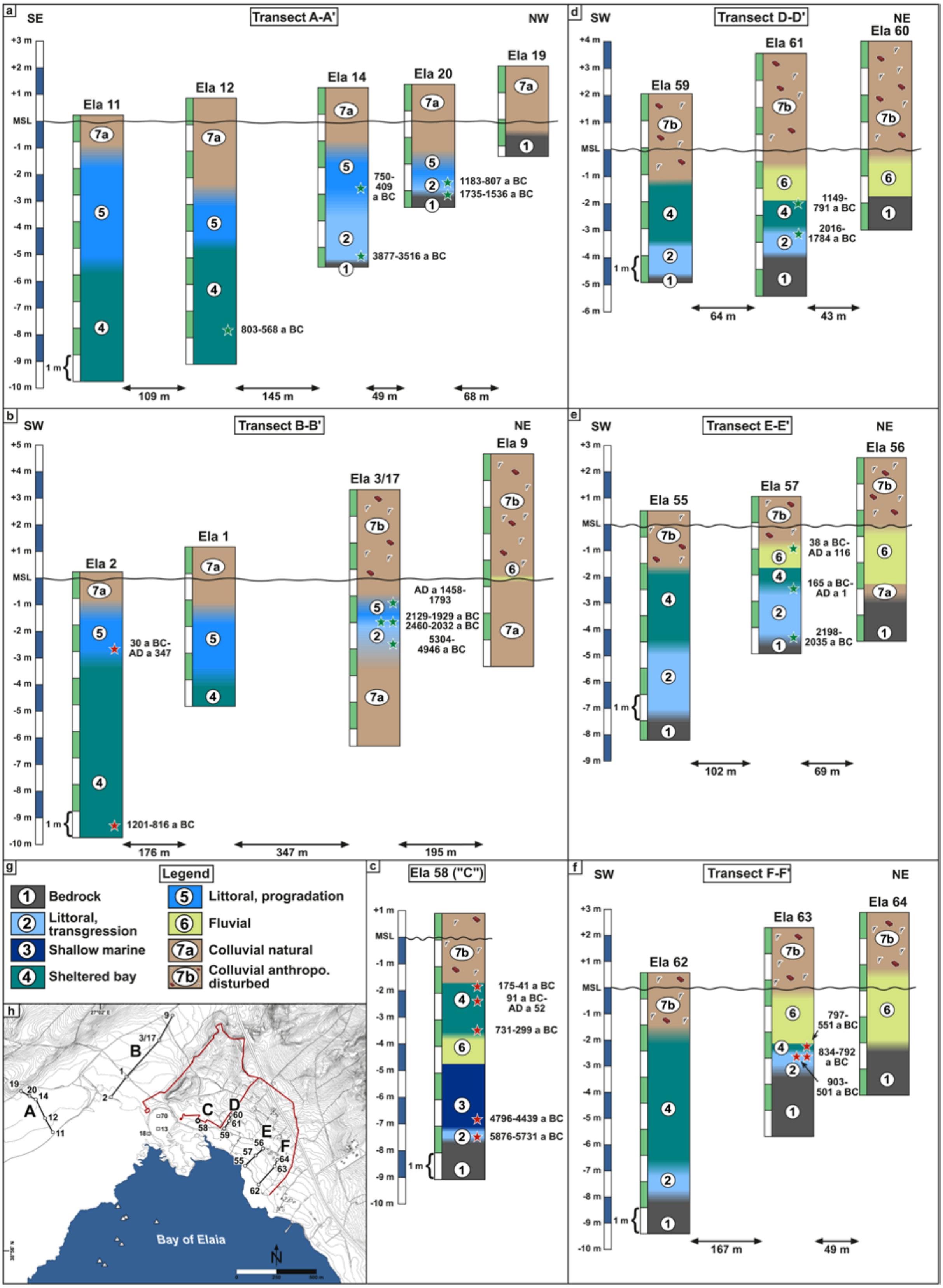
a
SE
Transect A-A'
NW
+3 m
+2 m
+1 m
MSL
-1 m
-2 m
-3 m
-4 m
-5 m
-6 m
-7 m
-8 m
-9 m
-10 m
1 m
Ela 11
Ela 12
Ela 14
Ela 20
Ela 19
750-409 a BC
3877-3516 a BC
1183-807 a BC
1735-1536 a BC
803-568 a BC
109 m
145 m
49 m
68 m
b
SW
Transect B-B'
NE
+5 m
Ela 2
Ela 1
Ela 3/17
Ela 9
30 a BC-AD a 347
1201-816 a BC
AD a 1458-1793
2129-1929 a BC
2460-2032 a BC
5304-4946 a BC
176 m
347 m
195 m
c
Ela 58 ("C")
175-41 a BC
91 a BC-AD a 52
731-299 a BC
4796-4439 a BC
5876-5731 a BC
d
SW
Transect D-D'
NE
+4 m
Ela 59
Ela 61
Ela 60
1149-791 a BC
2016-1784 a BC
64 m
43 m
e
SW
Transect E-E'
NE
Ela 55
Ela 57
Ela 56
38 a BC-AD a 116
165 a BC-AD a 1
2198-2035 a BC
102 m
69 m
f
SW
Transect F-F'
NE
Ela 62
Ela 63
Ela 64
797-551 a BC
834-792 a BC
903-501 a BC
167 m
49 m
g
Legend
1 Bedrock
2 Littoral, transgression
3 Shallow marine
4 Sheltered bay
5 Littoral, progradation
6 Fluvial
7a Colluvial natural
7b Colluvial anthropo. disturbed
h
A
B
C
D
E
F
Bay of Elaia
N

**Fig. 8.**

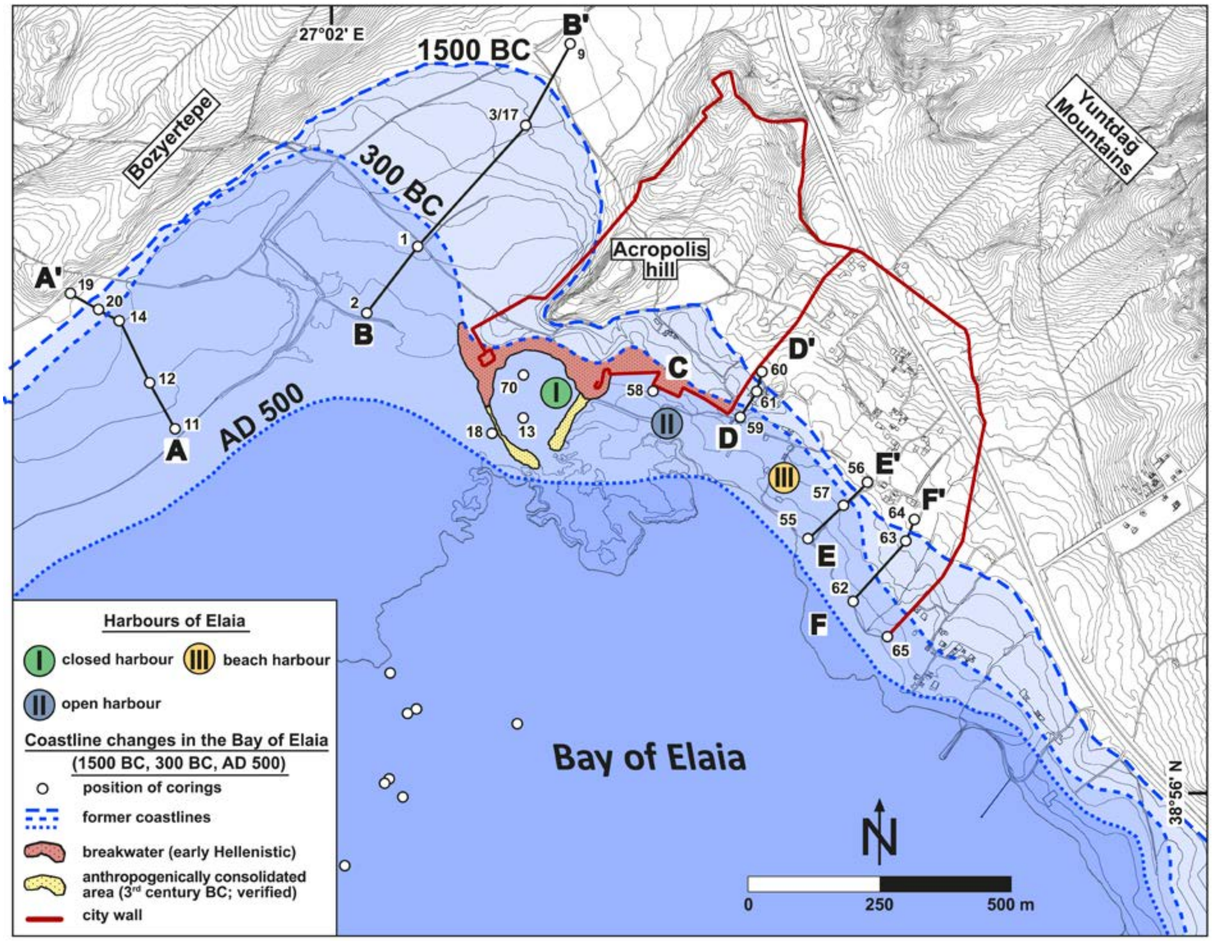
27°02' E
1500 BC
B'
9
3/17
Bozyertepe
300 BC
1
2
B
A'
19
20
14
12
11
A
AD 500
Acropolis hill
Yuntdağ Mountains
C
58
70
I
II
18
13
D'
60
61
D
59
III
56
E'
57
55
E
64
F'
63
62
F
65
Bay of Elaia
38°56' N
N
0
250
500 m
Harbours of Elaia
closed harbour
beach harbour
open harbour
Coastline changes in the Bay of Elaia (1500 BC, 300 BC, AD 500)
position of corings
former coastlines
breakwater (early Hellenistic)
anthropogenically consolidated area (3rd century BC; verified)
city wall

**Fig. 9.**

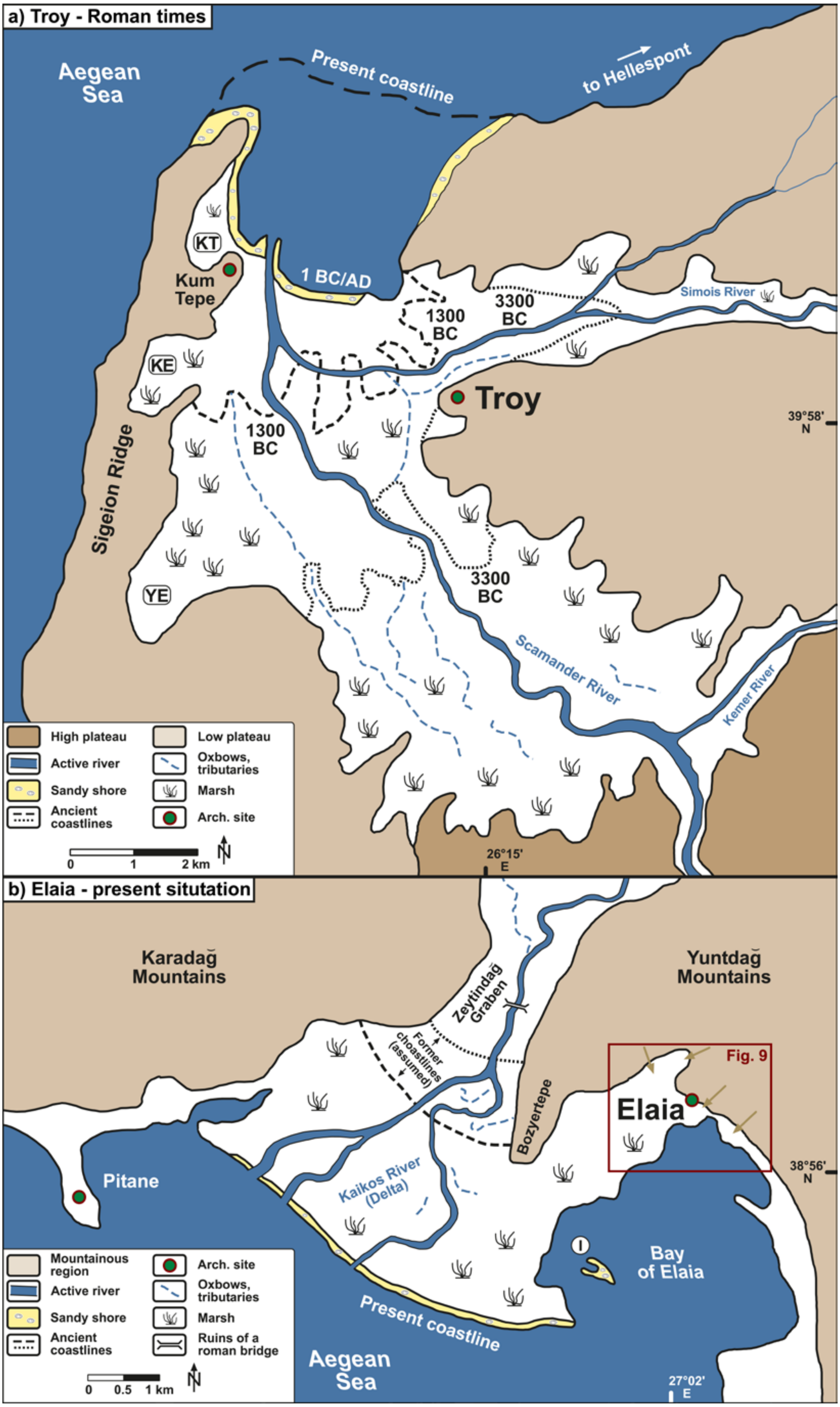
a) Troy - Roman times
Aegean Sea
Present coastline
to Hellespont
KT
Kum Tepe
1 BC/AD
1300 BC
3300 BC
Simois River
KE
Troy
39°58' N
1300 BC
Sigeion Ridge
3300 BC
YE
Scamander River
Kemer River
High plateau
Low plateau
Active river
Oxbows, tributaries
Sandy shore
Marsh
Ancient coastlines
Arch. site
0 1 2 km
N
26°15' E
b) Elaia - present situtation
Karadağ Mountains
Yuntdağ Mountains
Zeytindağ Graben
Former choastlines (assumed)
Fig. 9
Elaia
Bozyertepe
38°56' N
Pitane
Kaikos River (Delta)
I
Bay of Elaia
Mountainous region
Arch. site
Active river
Oxbows, tributaries
Sandy shore
Marsh
Ancient coastlines
Ruins of a roman bridge
0 0.5 1 km
N
Present coastline
Aegean Sea
27°02' E

**Fig. 10.**